

real radiofrequency pulses

Up to now the effects of rf pulses are described with neglect of further interactions (mainly chemical shift evolution) during the pulses. In this case the spin operators are rotated around the spin operator given by the pulse phase in the rotating frame.

In the following section we will analyze the more real situation where chemical shift evolution takes place during the action of pulses.

For a one spin system, any arbitrary spin state can be expressed by

$$\sigma(t) = c_x(t) \mathbf{I}_x + c_y(t) \mathbf{I}_y + c_z(t) \mathbf{I}_z$$

This state can be described by the corresponding coefficient vector:

$$\sigma(t) = [\mathbf{I}_x \mathbf{I}_y \mathbf{I}_z] \begin{bmatrix} c_x(t) \\ c_y(t) \\ c_z(t) \end{bmatrix}$$

To calculate the time development of the system it is sufficient to analyze the evolution of this coefficient vector.

The action of pulses with x- or y-phases and the larmor precession results in rotations of the coefficient vector around the corresponding axes. The rotation angle is given by $\phi = \omega \tau$

These rotations can be represented as matrices acting on the coefficient vector:

$$R_x = \begin{bmatrix} 1 & 0 & 0 \\ 0 & \cos \phi & -\sin \phi \\ 0 & \sin \phi & \cos \phi \end{bmatrix} = \begin{bmatrix} 1 & 0 & 0 \\ 0 & \cos \omega \tau & -\sin \omega \tau \\ 0 & \sin \omega \tau & \cos \omega \tau \end{bmatrix}$$

$$R_y = \begin{bmatrix} \cos \phi & 0 & \sin \phi \\ 0 & 1 & 0 \\ -\sin \phi & 0 & \cos \phi \end{bmatrix}$$

$$R_z = \begin{bmatrix} \cos \phi & -\sin \phi & 0 \\ \sin \phi & \cos \phi & 0 \\ 0 & 0 & 1 \end{bmatrix}$$

The evolution of the coefficient is then given by

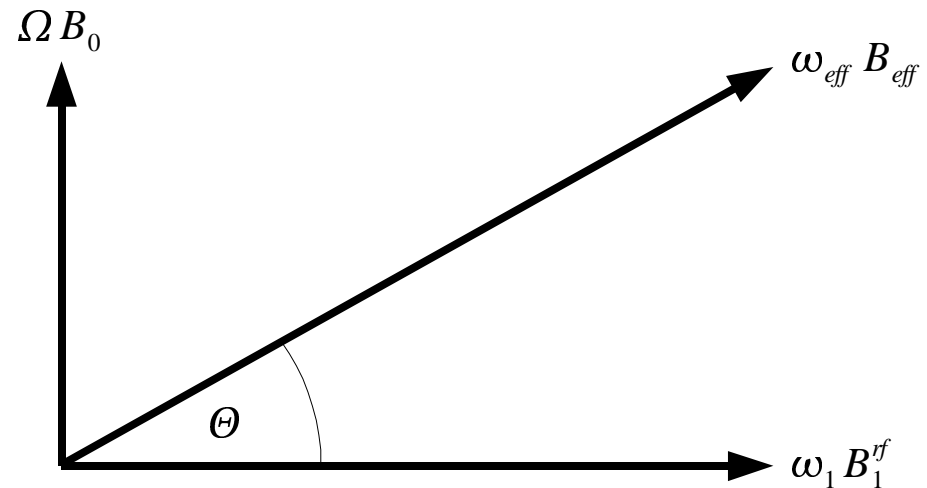
$$\begin{bmatrix} c_x(\tau) \\ c_y(\tau) \\ c_z(\tau) \end{bmatrix} = R_\alpha(\omega, \tau) \begin{bmatrix} c_x(0) \\ c_y(0) \\ c_z(0) \end{bmatrix}$$

Are two fields , e.g. rf-field and B_0 -field, active at the same time, an effective field results with direction and strength given by simple vector addition:

$$\omega_{eff} B_{eff} = \omega_1 B_1^{rf} + \Omega B_0$$

$$\omega_{eff} = \sqrt{\omega_1^2 + \Omega^2}$$

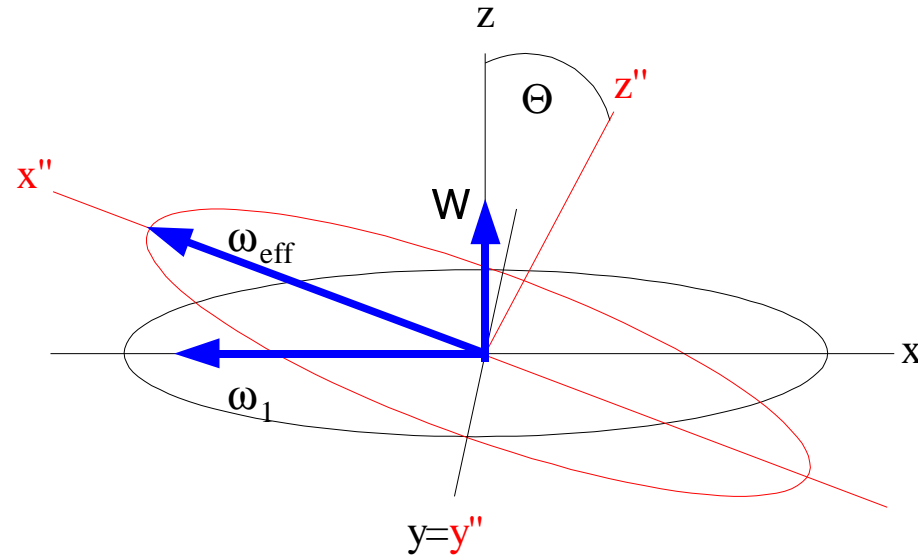
$$\cos \Theta = \frac{\omega_1}{\omega_{eff}}$$



The magnetization precesses now around the effective field B_{eff} with a frequency ω_{eff} .

The precession around the effective field can be described by three subsequent rotations:

1. rotation around y (assumption: x-pulse) with an angle $-\Theta$,
2. rotation around x'' with an angle $\phi = \omega_{eff} \tau$
3. rotation around $y = y''$ with an angle Θ



$$\begin{bmatrix} c_x(\tau) \\ c_y(\tau) \\ c_z(\tau) \end{bmatrix} = R_y(\Theta) R_x(\phi) R_y(-\Theta) \begin{bmatrix} c_x(0) \\ c_y(0) \\ c_z(0) \end{bmatrix} = \begin{bmatrix} \cos \Theta & 0 & \sin \Theta \\ 0 & 1 & 0 \\ -\sin \Theta & 0 & \cos \Theta \end{bmatrix} \begin{bmatrix} 1 & 0 & 0 \\ 0 & \cos \phi & -\sin \phi \\ 0 & \sin \phi & \cos \phi \end{bmatrix} \begin{bmatrix} \cos \Theta & 0 & -\sin \Theta \\ 0 & 1 & 0 \\ \sin \Theta & 0 & \cos \Theta \end{bmatrix} \begin{bmatrix} c_x(0) \\ c_y(0) \\ c_z(0) \end{bmatrix}$$

multiplying all three rotation matrices result in the general rotation matrix describing the action of an arbitrary rectangular pulse with x-phase with simultaneous presence of Larmor precession around the z-axis:

$$R_p(\Omega, \omega_1, \tau) = \begin{bmatrix} \cos^2 \Theta + \cos \phi \sin^2 \Theta & -\sin \phi \sin \Theta & -\cos \Theta \sin \phi (1 - \cos \phi) \\ \sin \phi \sin \Theta & \cos \phi & -\sin \phi \cos \Theta \\ \cos \Theta \sin \phi (1 - \cos \phi) & \sin \phi \cos \Theta & \sin^2 \Theta + \cos \phi \cos^2 \Theta \end{bmatrix}$$

In the case of an arbitrary phase α of the rf-field in the x,y plane an additional rotation around the z-axis is necessary:

$$R_p(\Omega, \omega_1, \tau, \alpha) = R_z(\alpha) R_p(\Omega, \omega_1, \tau) R_z(-\alpha)$$

—————▶ With these rotation matrices it is possible to calculate the excitation profile of any given pulse.

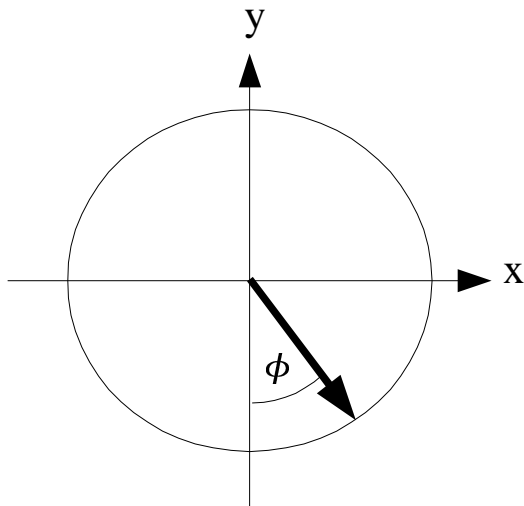
For the action of rf-pulses three rotations are important:

1. Excitation, rotating of z-magnetization into the transverse plane,
this is the standard on-resonant 90° pulse

$$\mathbf{I}_z \xrightarrow{\omega_1 \tau \mathbf{I}_x + \Omega_I \tau \mathbf{I}_z} c_x(\tau) \mathbf{I}_x + c_y(\tau) \mathbf{I}_y + c_z(\tau) \mathbf{I}_z$$

$$\text{with } \omega_1 \tau = \frac{\pi}{2} \quad \text{for} \quad \Omega_I = 0 \quad \text{result in} \quad \begin{bmatrix} c_x(\tau) \\ c_y(\tau) \\ c_z(\tau) \end{bmatrix} = \begin{bmatrix} 0 \\ -\sin(\omega_1 \tau) \\ \cos(\omega_1 \tau) \end{bmatrix} = \begin{bmatrix} 0 \\ -1 \\ 0 \end{bmatrix}$$

Instead of viewing the cartesian der x,y,z components of the magnetization the excitation profile of an excitation pulse can be deccribed by the amplitude and phase of the resulting transverse magnetization:



$$M_{transversal} = M_0 \sqrt{c_x^2(\tau, \Omega_I) + c_y^2(\tau, \Omega_I)}$$

$$\tan(\phi, \Omega_I) = -\frac{c_x(\tau, \Omega_I)}{c_y(\tau, \Omega_I)}$$

2. inversion rotation from z nach -z (or opposite direction) by a 180° pulse with x- or y-phase
3. refocusing rotation from x to -x by a 180° pulse with y-phase, or
rotation from y nach -y by a 180° pulse with x-phase

The influence of larmor precession during the action of the pulse is not the same in the case of inversion compared to refocusing. Consequently a 180° pulse of same duration shows different profiles for both rotations.

For the inversion the pulse phase does not play a role, because the resulting transverse magnetization comes from pulse imperfections and should be suppressed by proper methods-

A refocusing pulse acts on transverse magnetization, therefore the phase of the pulse is important.

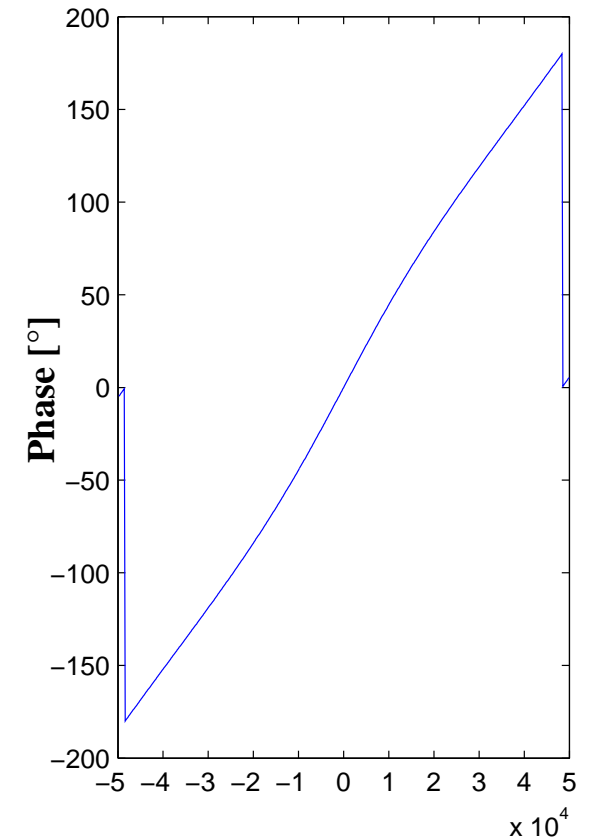
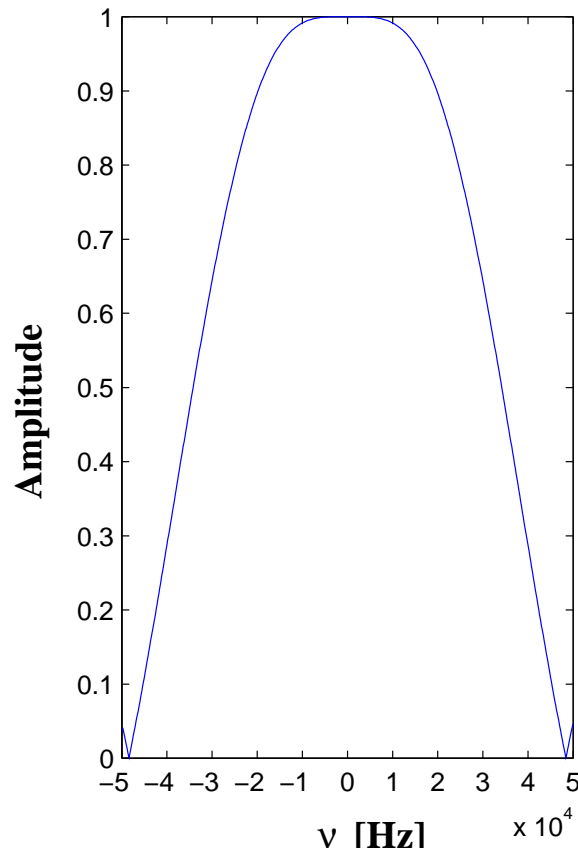
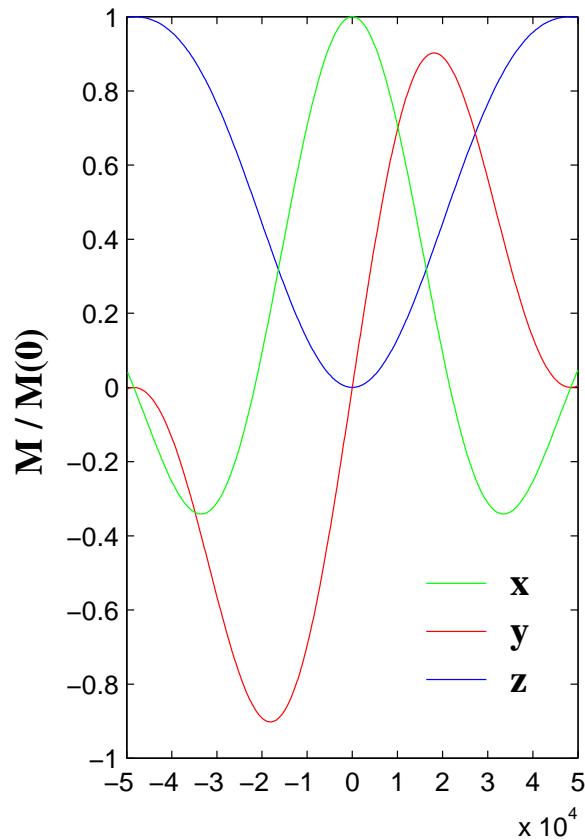
The following rule is valid:

a good refocusing pulse is also a good inversion pulse, but
a good inversion pulse might be a worse refocusing pulse

Excitation profile of a 90° rectangular pulse

pulse duration 20 μs \rightarrow $\nu_{rf} = \frac{\gamma B_1}{2\pi} = \frac{1}{4\tau_{90^\circ}} = 12500 \text{ Hz}$

M(x,y,z) nach Puls



Excitation in the region $|\nu| < \nu_{rf} \rightarrow \sqrt{M_x^2 + M_y^2}$

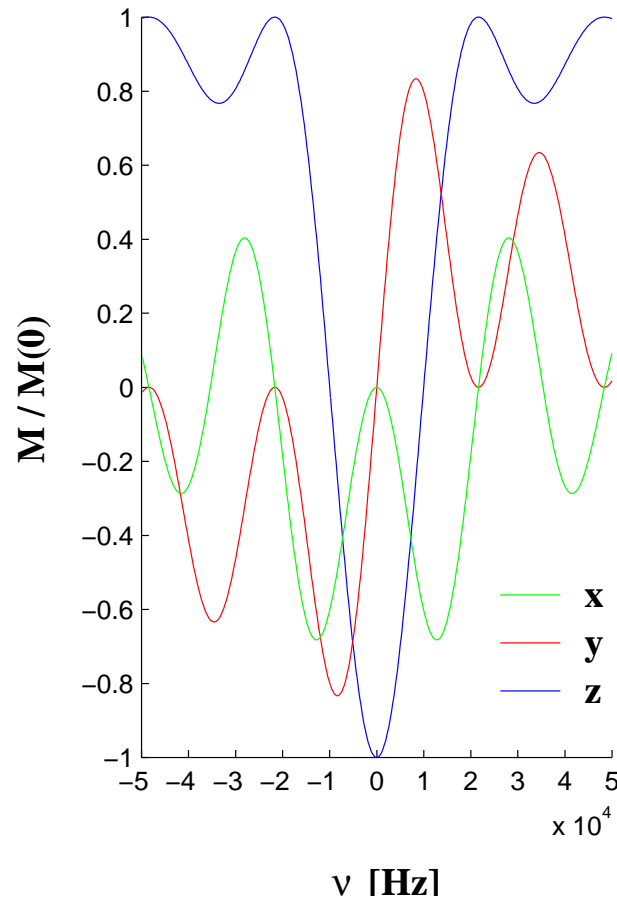
Excitation in the region $|\nu| < 1.5 \nu_{rf} \rightarrow \sqrt{M_x^2 + M_y^2} / M_0 > 0.91$

1. excitation 'zero' ($M_{x,y} = 0$) at $\nu_{zero} \approx \frac{0.97}{\tau_{90^\circ}}$

Inversionprofile of a 180° rectangular pulse

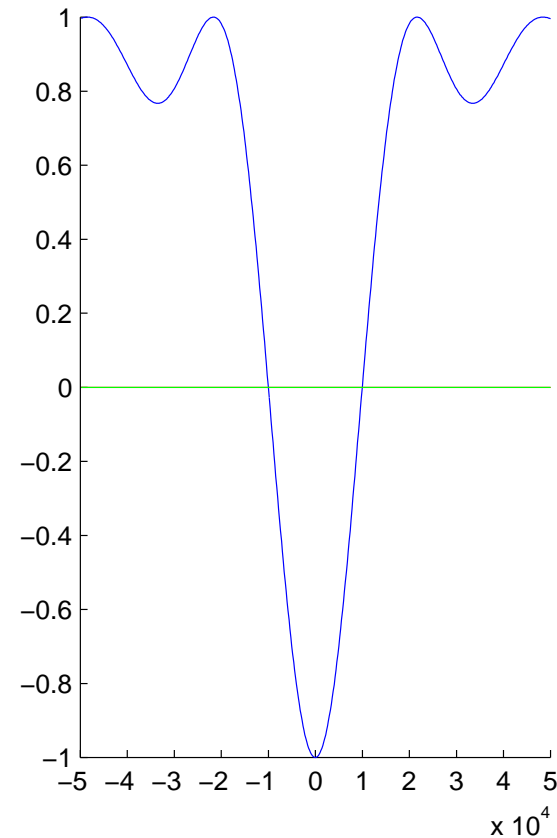
pulse duration 40 μs \longrightarrow $\nu_{rf} = \frac{\gamma B_1}{2\pi} = \frac{1}{4\tau_{90^\circ}} = 12500 \text{ Hz}$

M(x,y,z) nach Puls



M(x,y,z) nach Phasenzyklus

1. Experiment: $\phi = +x$, rec = +
2. Experiment: $\phi = -x$, rec = +



inversion in the region $|\nu| < 0.25 \nu_{rf} : M_z \rightarrow -M_z > 0.90$

inversion in the region $|\nu| < 0.5 \nu_{rf} : M_z \rightarrow -M_z > 0.55$

1. inversion 'zero' ($M_z = 0$) at $\nu_{zero} \approx \frac{0.87}{\tau_{180^\circ}}$

Refocusingprofile (y \longrightarrow -y) of a 180° rectangular pulse

pulse duration 40 μ s \longrightarrow $\nu_{rf} = \frac{\gamma B_1}{2\pi} = \frac{1}{4\tau_{90^\circ}} = 12500 \text{ Hz}$

M(x,y,z) nach Phasenzyklus

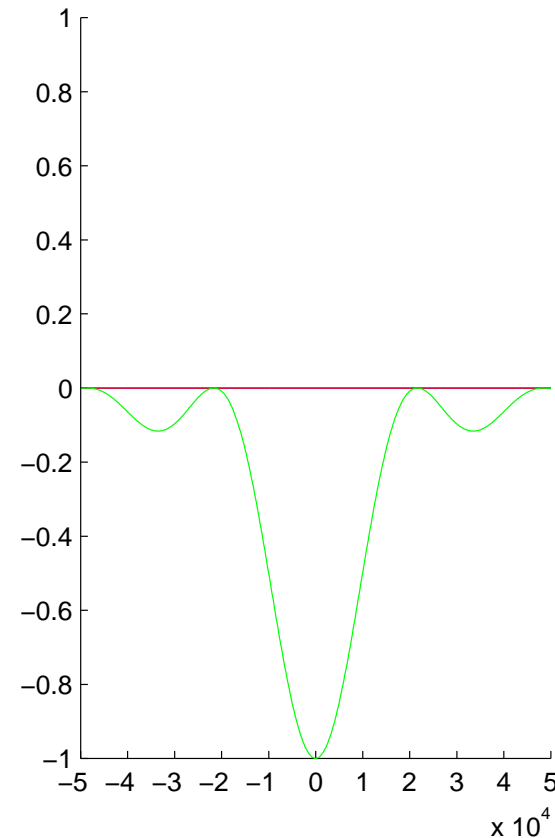
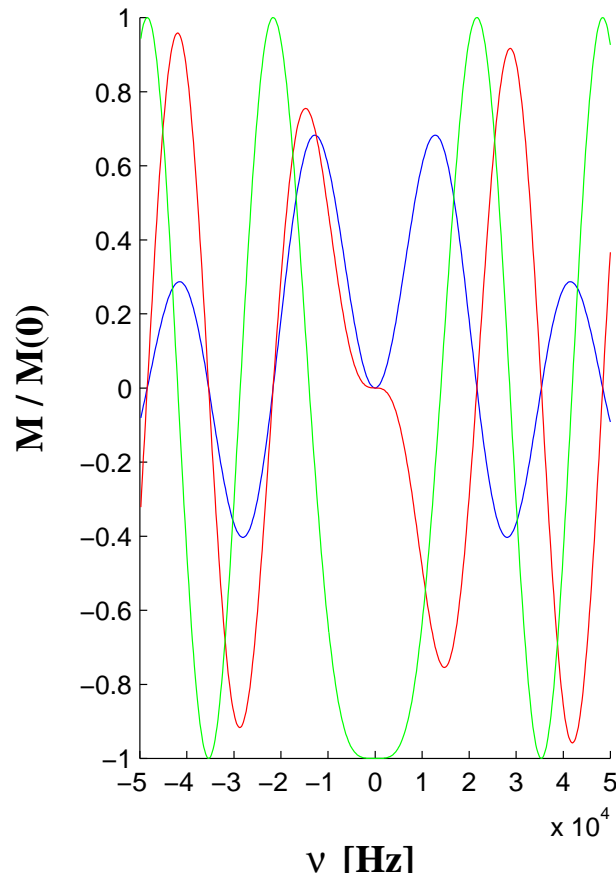
1. Experiment: $\phi = +x$, rec = +

2. Experiment: $\phi = -x$, rec = +

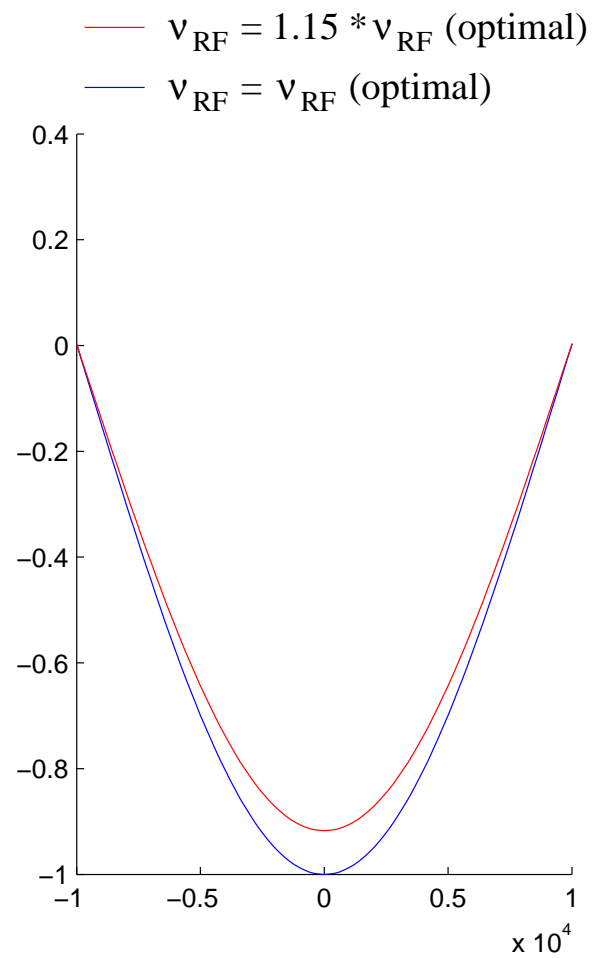
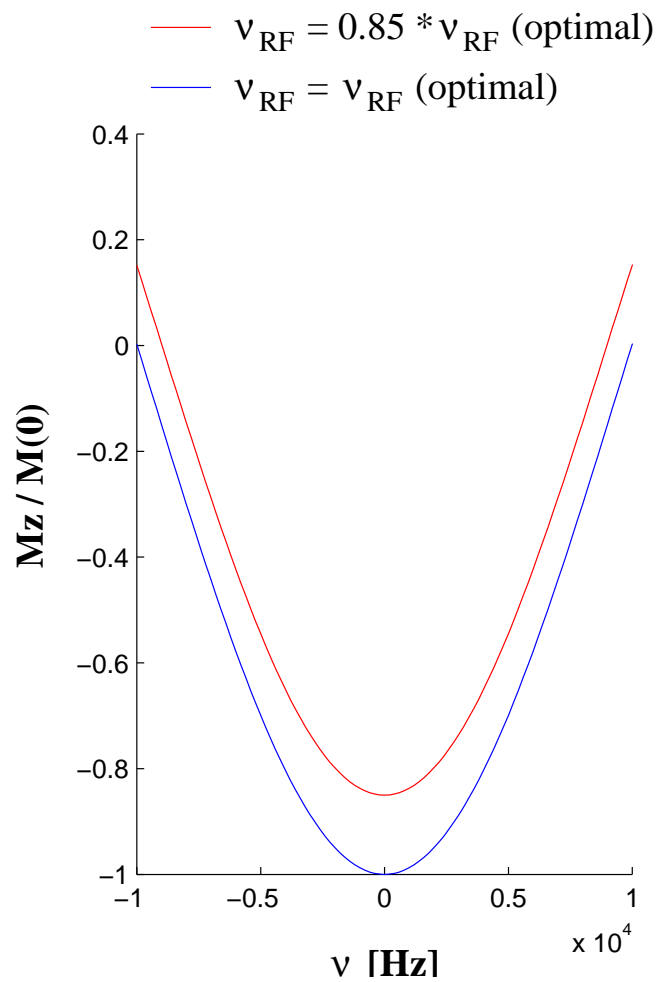
2. Experiment: $\phi = y$, rec = -

2. Experiment: $\phi = -y$, rec = -

M(x,y,z) nach Puls

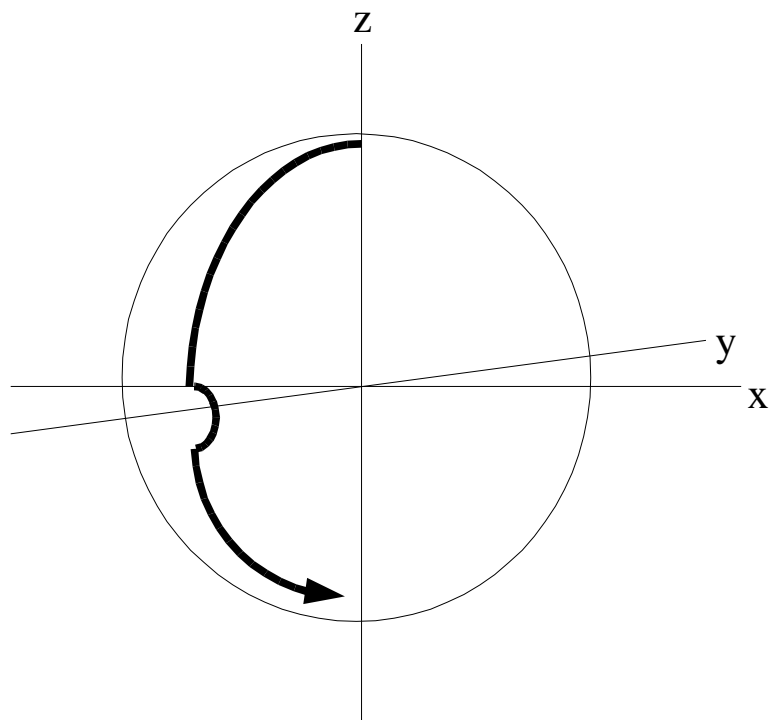


bad calibrated 180° pulse

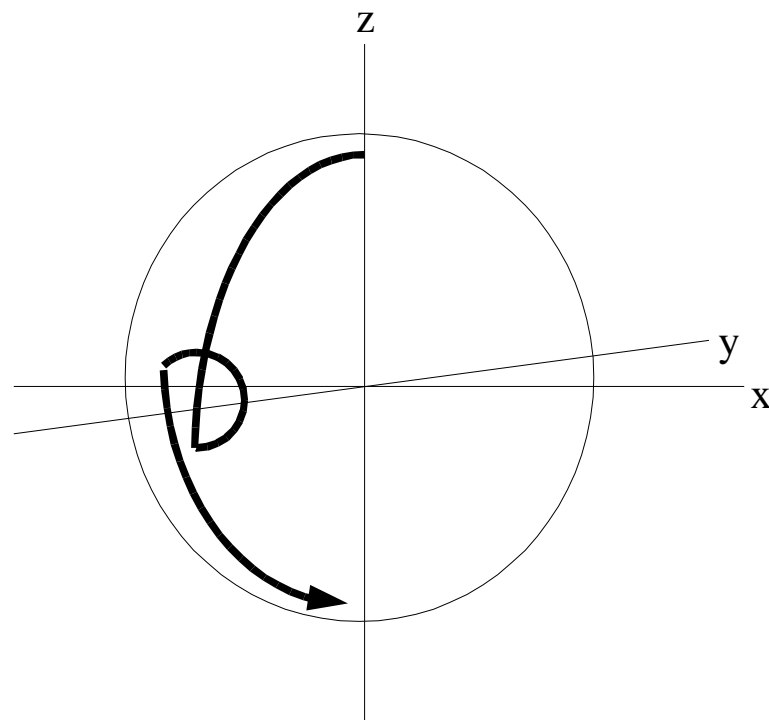


Action of a $90^\circ(x) - 180^\circ(y) - 90^\circ(x)$ composite pulse for inversion

pulse length too short

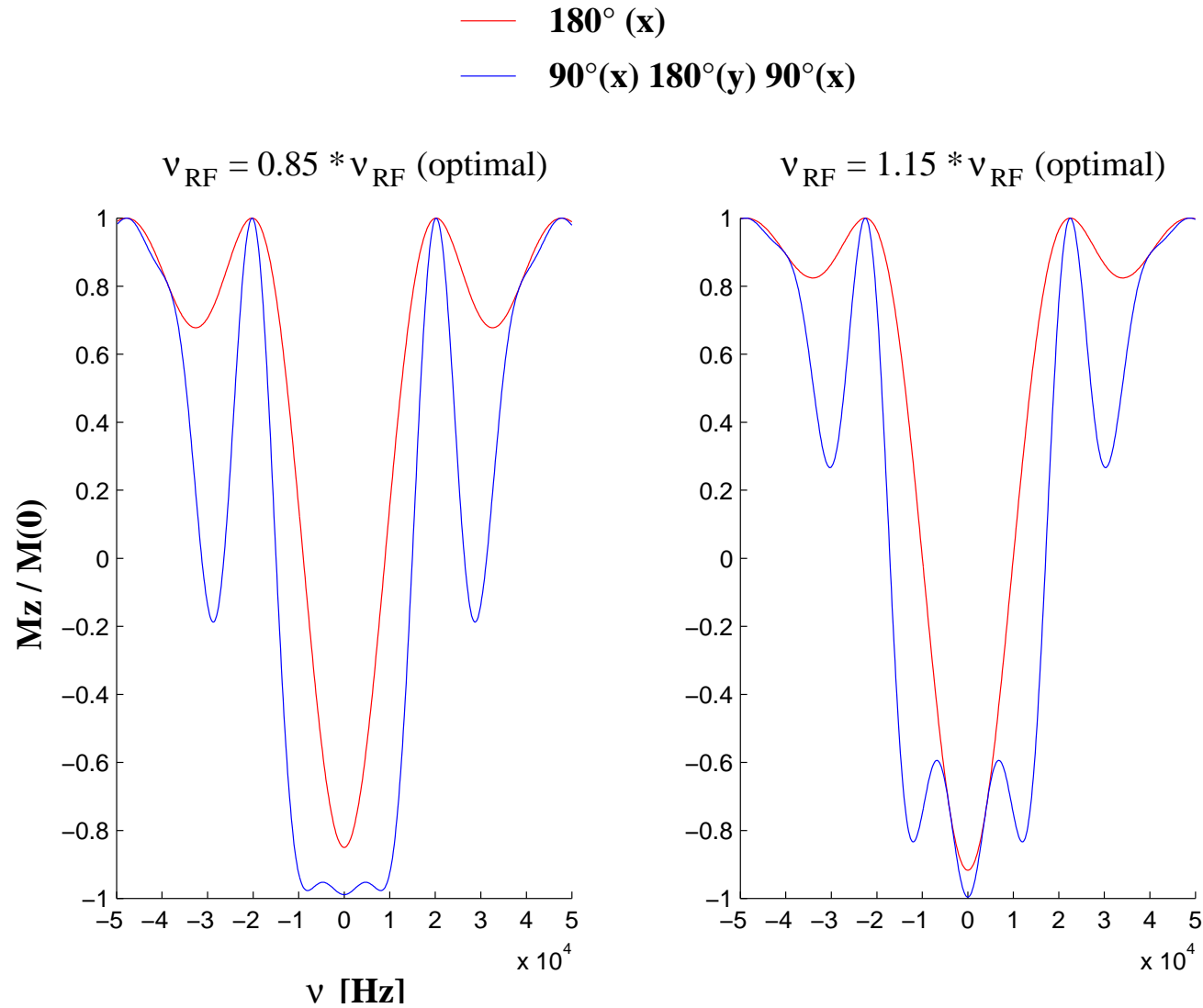


pulse length too long

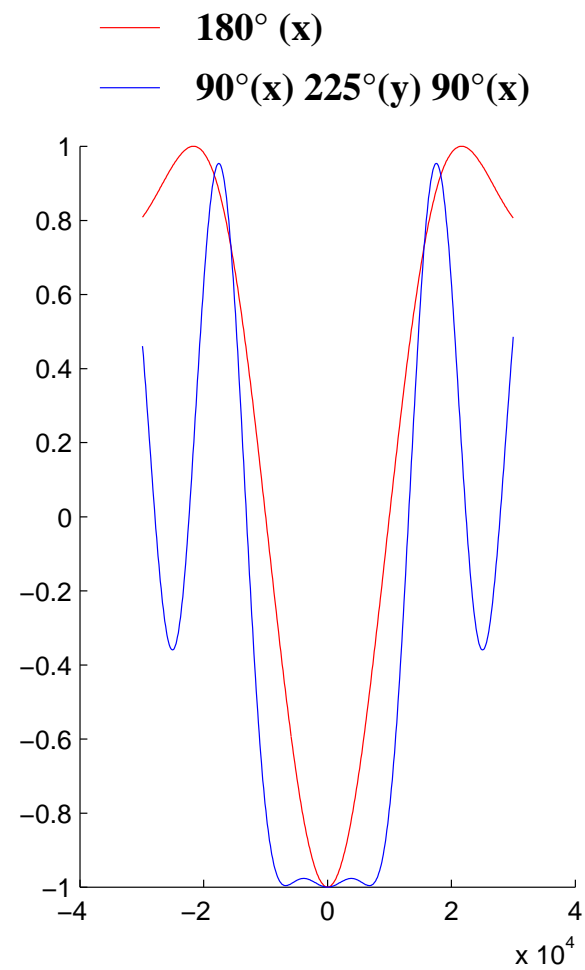
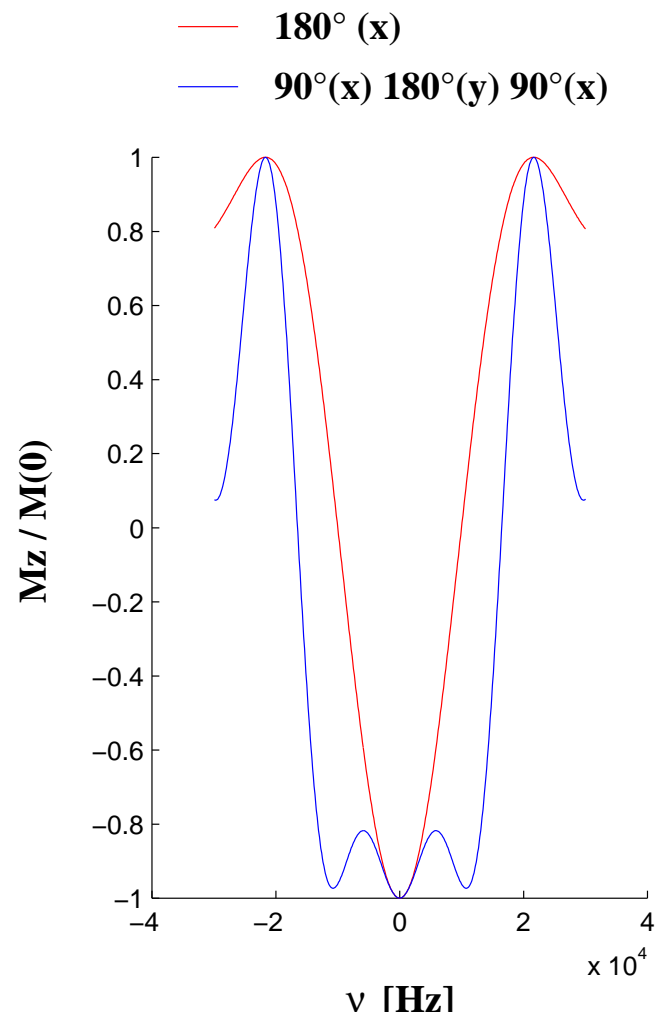


—————▶ composite pulse compensates the bad calibration to a large extent

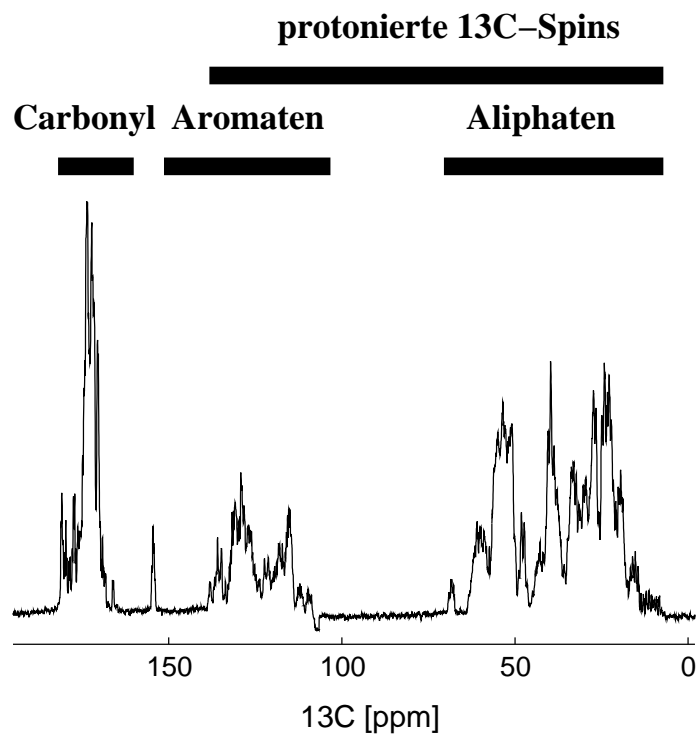
Inversion profile of a 'bad' calibrated $90^\circ(\text{x})$ $180^\circ(\text{y})$ $90^\circ(\text{x})$ composite pulse



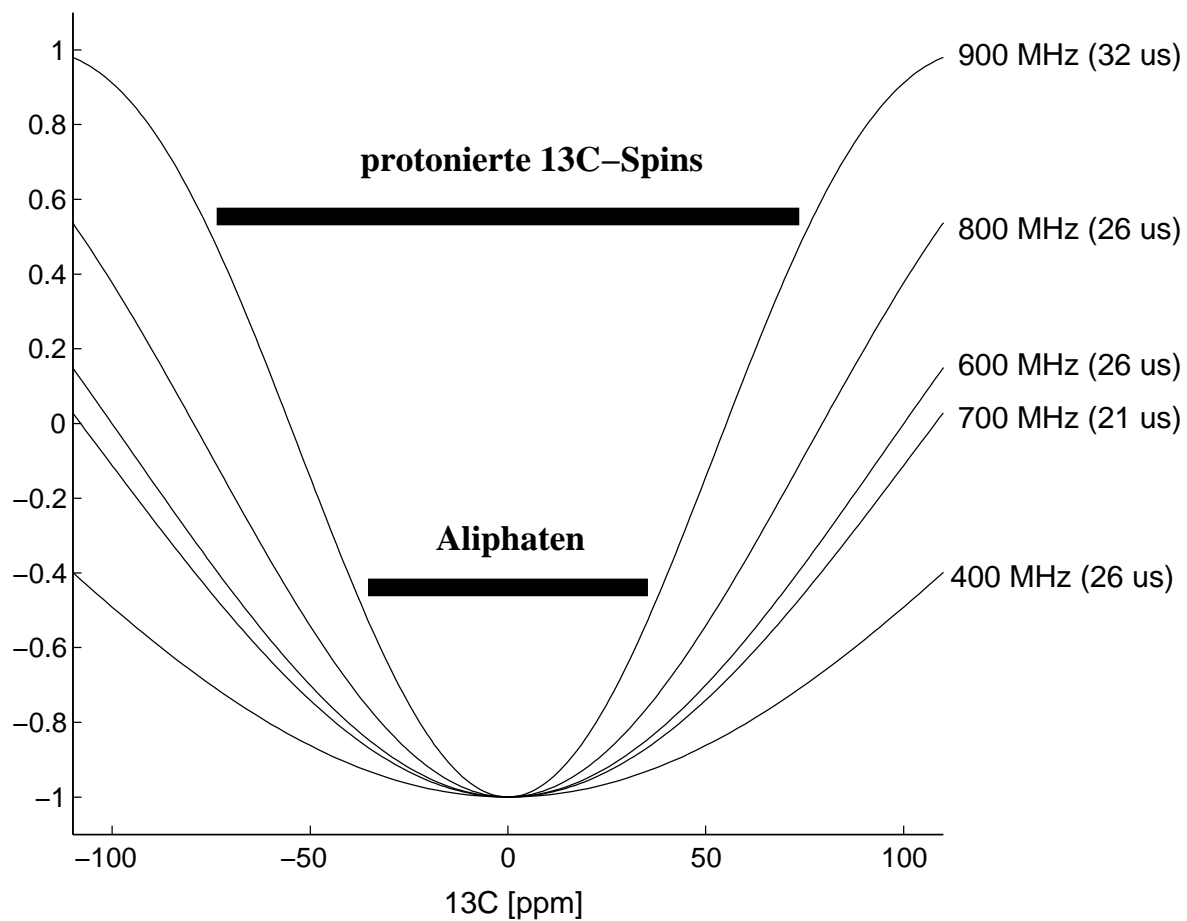
Inversion profile of a correct calibrated composite pulse



^{13}C NMR on proteins and real pulses



Inversionsprofil eines high-power ^{13}C 180° Pulses



The well separated regions of $^{13}\text{C}'$ and $^{13}\text{C}^{\alpha}$ chemical shifts in proteins allow the selective rotations by proper selected pulses.

A prominent method is to choose the durations of 90° and 180° pulses that they only excite only one of both regions, while the excitation profile of the applied pulse shows an excitation minimum in the other frequency range.

A 90° pulse has a first excitation minimum at ca. $0.97 / t$,
a 180° pulse (inversion) has a first minimum at ca. $0.87 / t$

The center of the $^{13}\text{C}'$ resonances lies around 175 ppm, that of the $^{13}\text{C}^{\alpha}$ spins around 56 ppm.

For a 600 MHz spectrometer the following pulse lengths should be used:

$$\tau_{90} = \frac{0.97}{119 \times 151 \text{ Hz}} = 54 \mu s$$
$$\tau_{180} = \frac{0.87}{119 \times 151 \text{ Hz}} = 48 \mu s$$

Remark: a 108 ms long 180° pulse has a too narrow inversion profile to be used for protein triple resonance experiments.

Amplitude- and phasemodulated pulses

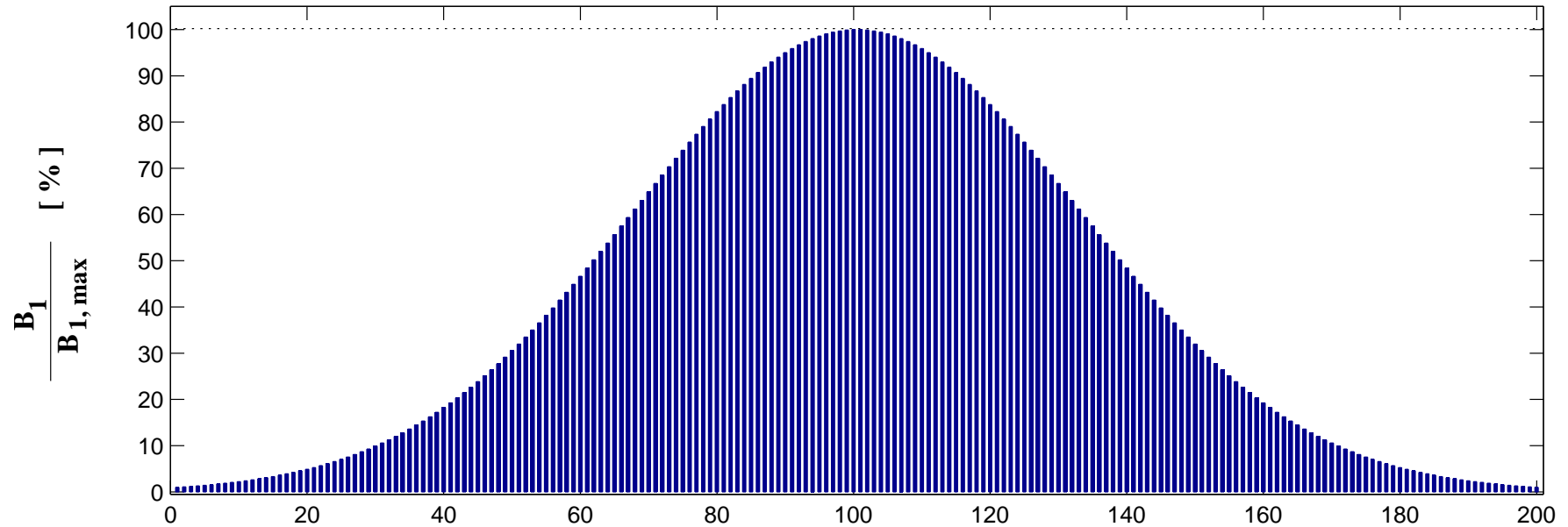
modern spectrometer allow not only using rectangular pulses, that means a constant amplitude during the pulse, but also pulses with variable amplitude and phase during the pulse can be realized.

With these 'shaped' pulses very designed excitation profiles can be achieved.

These pulses are realized by a series of very short rectangular pulses with different amplitudes and phases.

The time resolution of each pulse steps is around 50 ns on modern spectrometers.

Example: Gauß shape like puls, consisting of 200 short rectangular pulses



Calculation of the excitation profile of an amplitude modulated pulse

For a pulse consisting of N short rectangular pulses with equal length and variable amplitude A_i (in the range of $0.0 - 1.0 * \omega_1(\text{max})$), the excitation profile can be calculated (numerically) by subsequent application of the corresponding rotation matrices for the individual short rectangular pulses acting on the actual states of the magnetization:

$$\tau_p = N \cdot \Delta \tau$$

$$M(\tau_p) = \left\{ \prod_{i=1}^N R(\omega_1^i, \Delta t, \phi_i, \Omega) \right\} M(0)$$

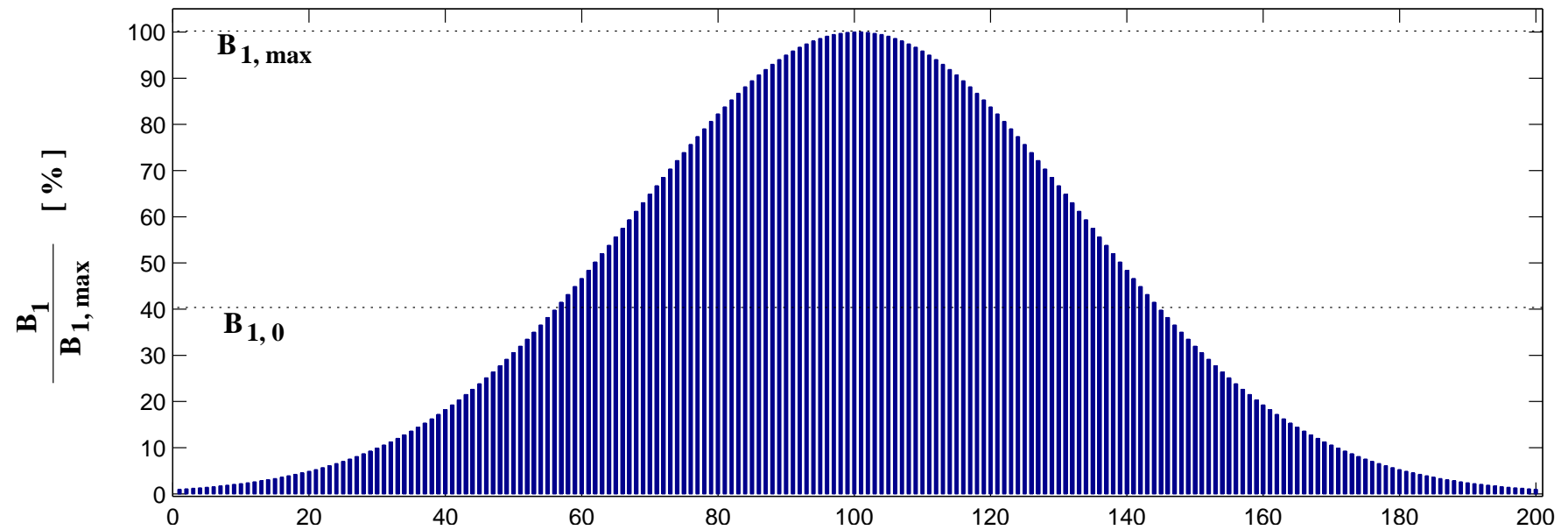
The onresonant pulse angle in the case of an amplitude modulated pulse (phase = 180° corresponds to a negative amplitude) is given by

$$\alpha = \sum_{i=1}^N \alpha_i \quad \text{mit} \quad \alpha_i = \omega_1^i \Delta \tau$$

Using the integral ratio (= ratio between the overall amplitude of a rectangular pulse with equal length and ω_1^0 and the integrated amplitude of the shaped pulse) and the onresonant pulse angle α the necessary rf field strength ω_1^{max} can be calculated:

$$\text{Int.Ratio} = \frac{1}{\sum_{i=1}^N A_i} \quad \omega_1^0 = \frac{\alpha}{\tau_p} \quad \longrightarrow \quad \omega_1^{\text{max}} = \frac{\omega_1^0}{\text{Int.Ratio}} \quad \omega_i = A_i \omega_1^{\text{max}}$$

Example: Gauß-like 90° pulse



$$Int.Ratio=0.40997$$

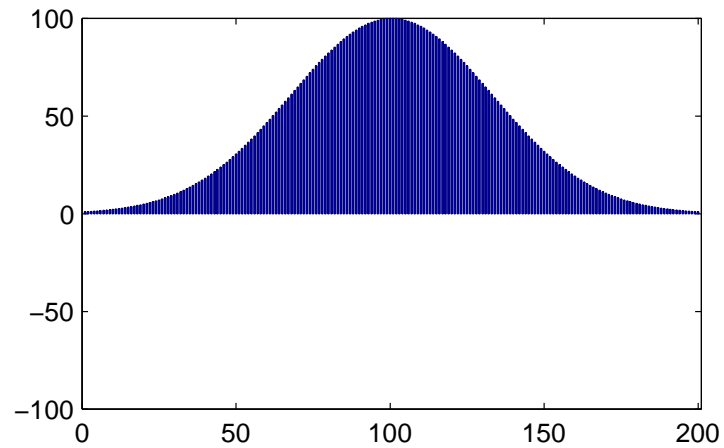
$$\tau_p=512\,\mu s$$

$$\frac{\omega_1^0}{2\pi}=488.3\,Hz$$

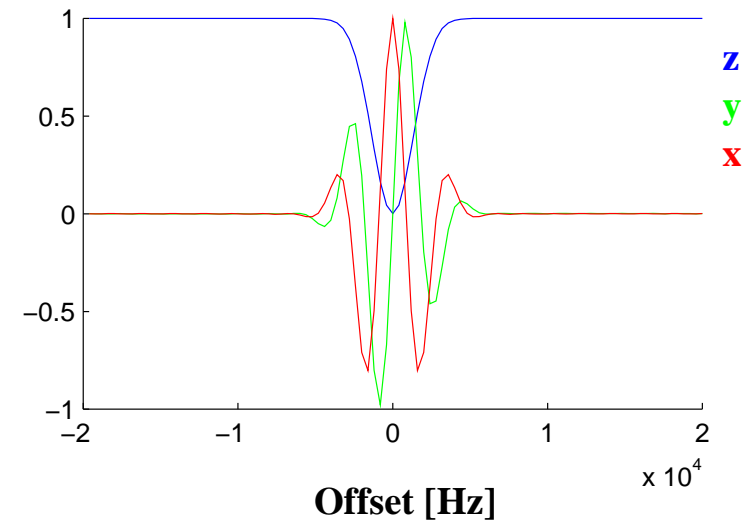
$$\frac{\omega_1^{\max}}{2\pi}=1191.0\,Hz \quad (\text{corresponds to a } 210\,\mu s \text{ } 90^\circ \text{ rectangular pulse})$$

Excitation profile of the Gauss pulse (90° , 512 ms)

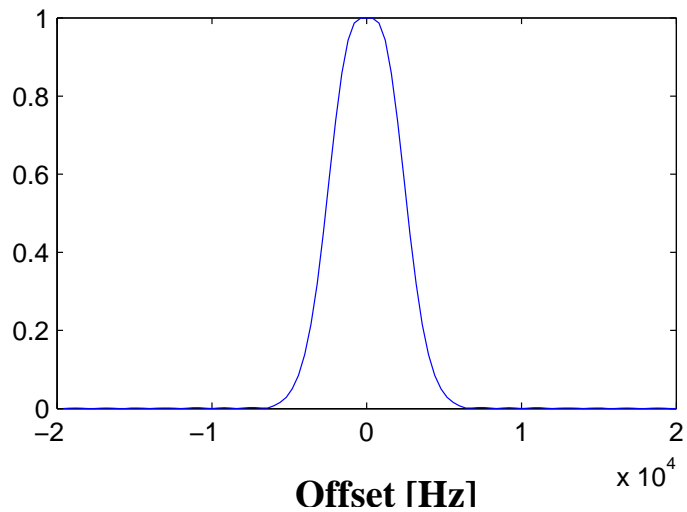
Pulsamplitude



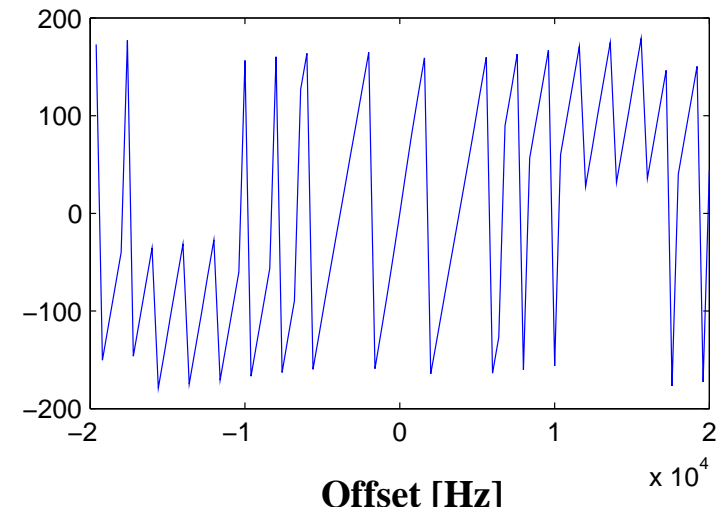
Anregungsprofil nach $90^\circ(y)$ Puls

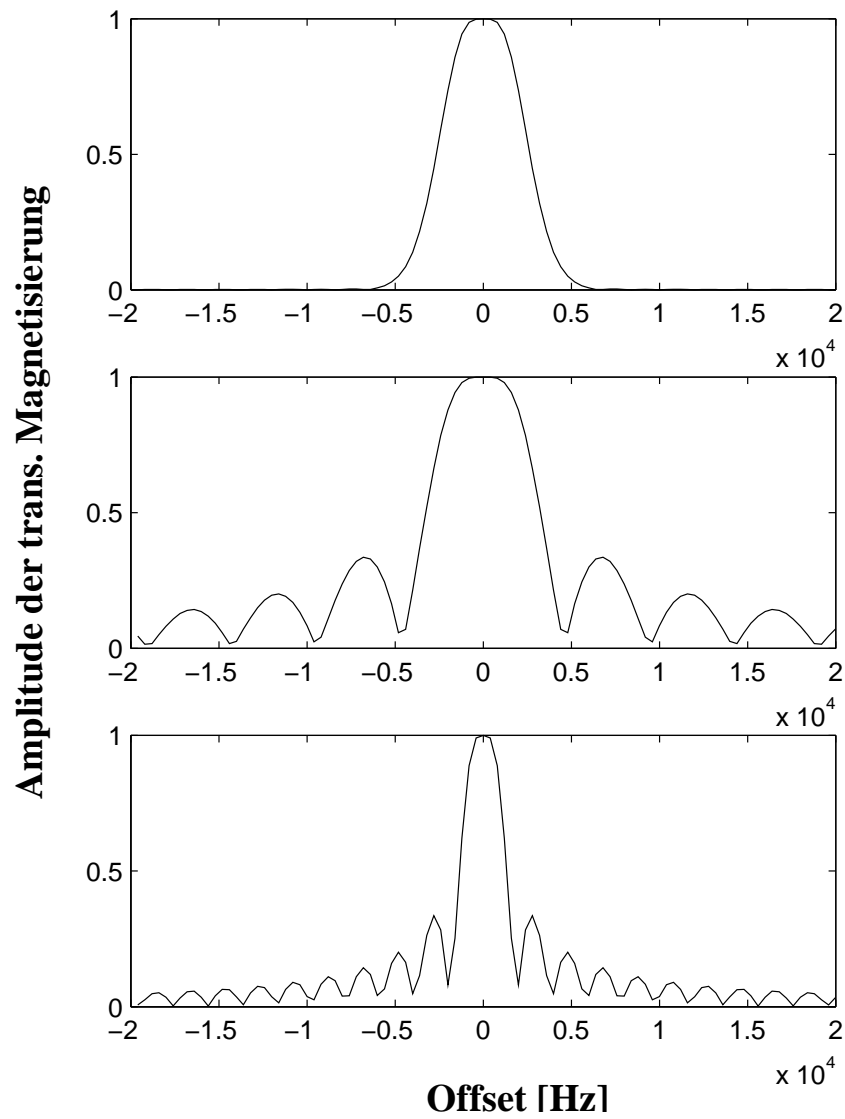


Amplitude der transv. Magnetisierung



Phase der transvers. Magnetisierung





Gauss-Puls, 512 μ s

$$\gamma B_{1, \max} = 1190 \text{ Hz}$$

Rechteck-Puls, 210 μ s

$$\gamma B_{1, \max} = 1190 \text{ Hz}$$

Rechteck-Puls, 512 μ s

$$\gamma B_{1, \max} = 488 \text{ Hz}$$

Summary: Comparison of a gauss-shape pulse with a rectangular pulse

In contrast to the rectangular pulse the Gauss-shape pulse exhibits the following features

At the same B_1^{max} the Gauss-like pulse exhibits a more narrow excitation profile

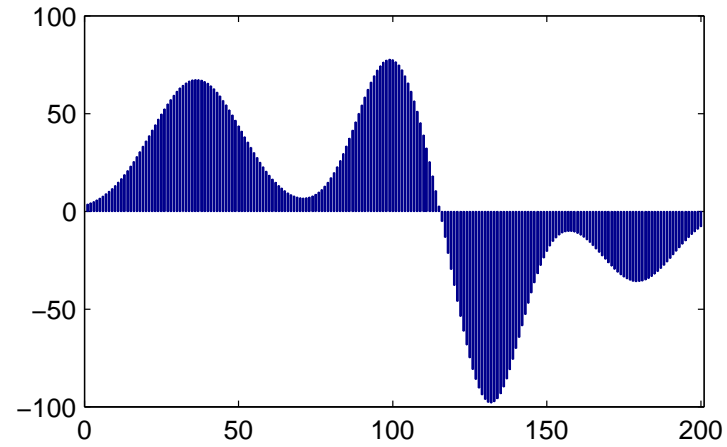
The Gauss-shape pulse shows up no further excitation bands outside the central band.

- The rectangular pulse is better for exciting a broader frequency band at a given rf field strength
- The Gauss-shape pulse is better for a more selective excitation band at a given rf field strength

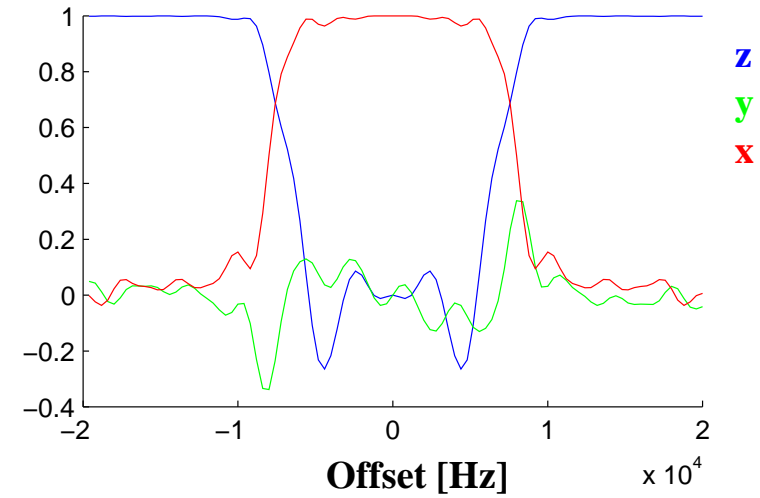
Excitation profile of a 90° G4 pulse (Gaussian cascade), 512 ms

—————➤ nearly top hat like excitation

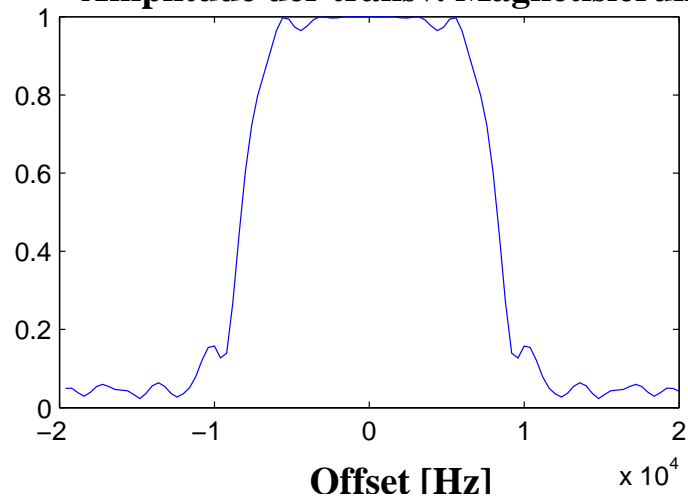
Pulsamplitude



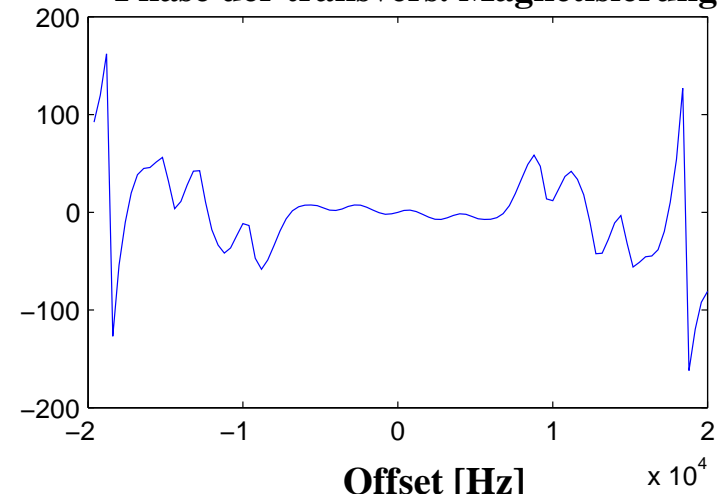
Anregungsprofil nach 90°(y) Puls



Amplitude der transv. Magnetisierung

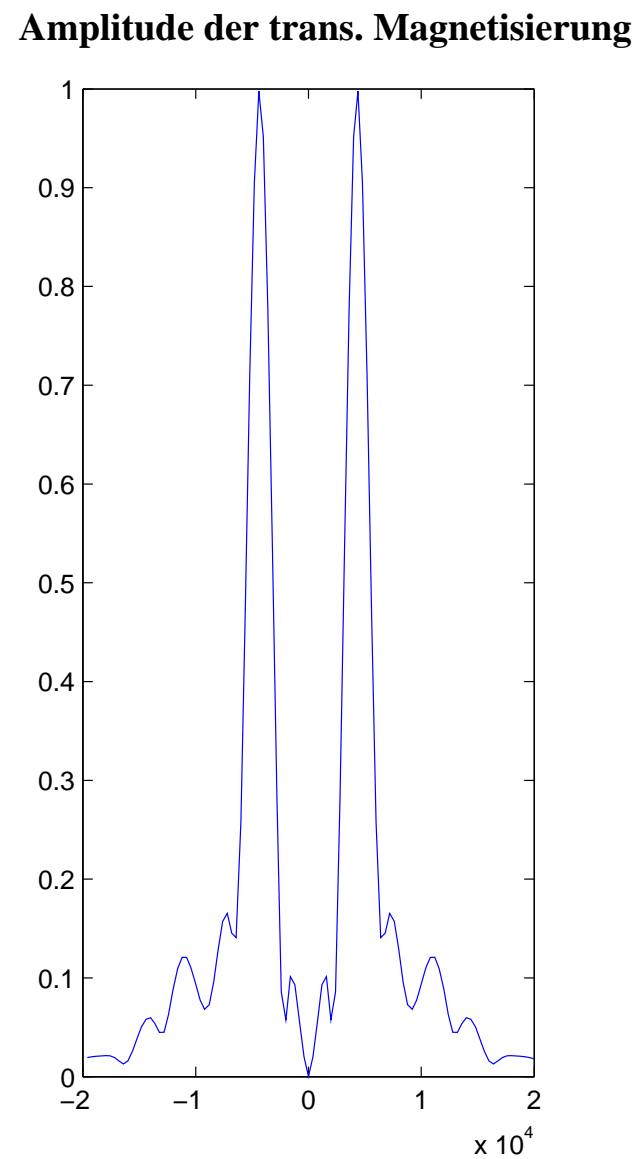
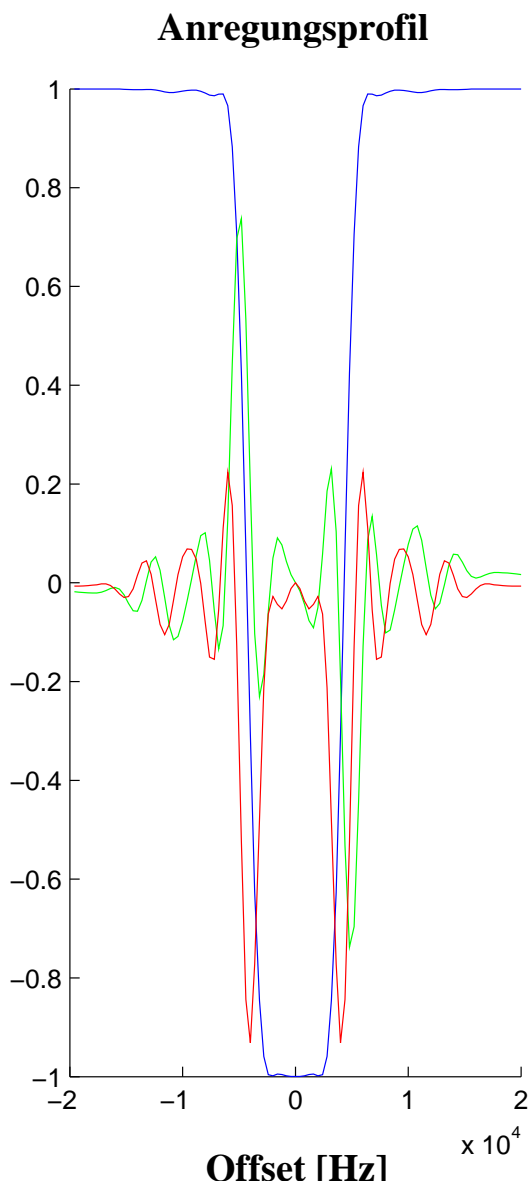
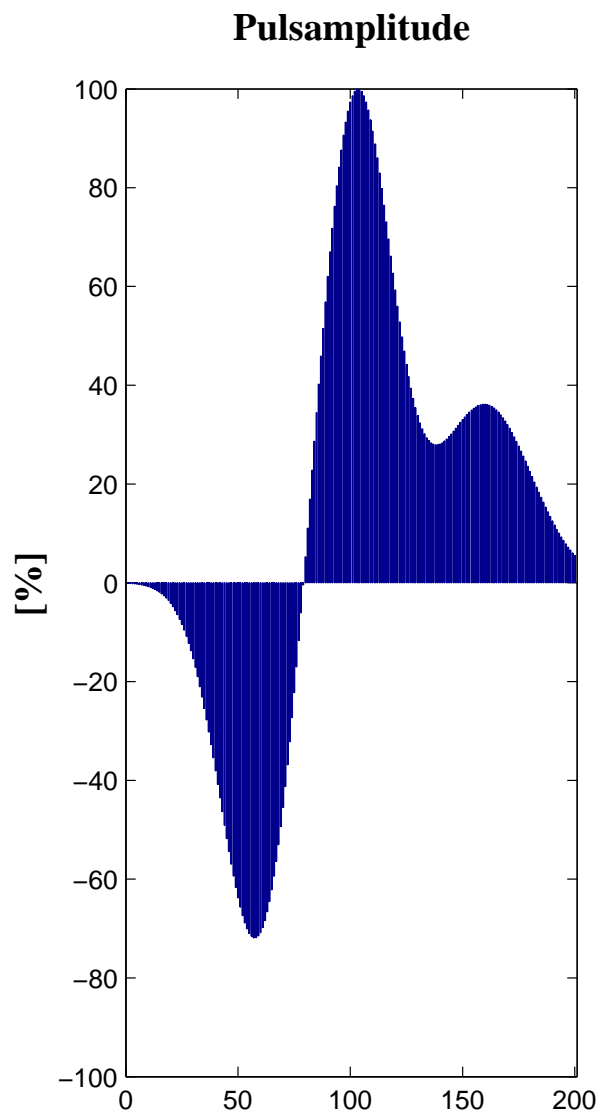


Phase der transvers. Magnetisierung



Inversion profile of 180° G3 pulse (Gaussian cascade, 512 ms)

→ nearly top hat like inversion



Coherence order and coherence transfer selection

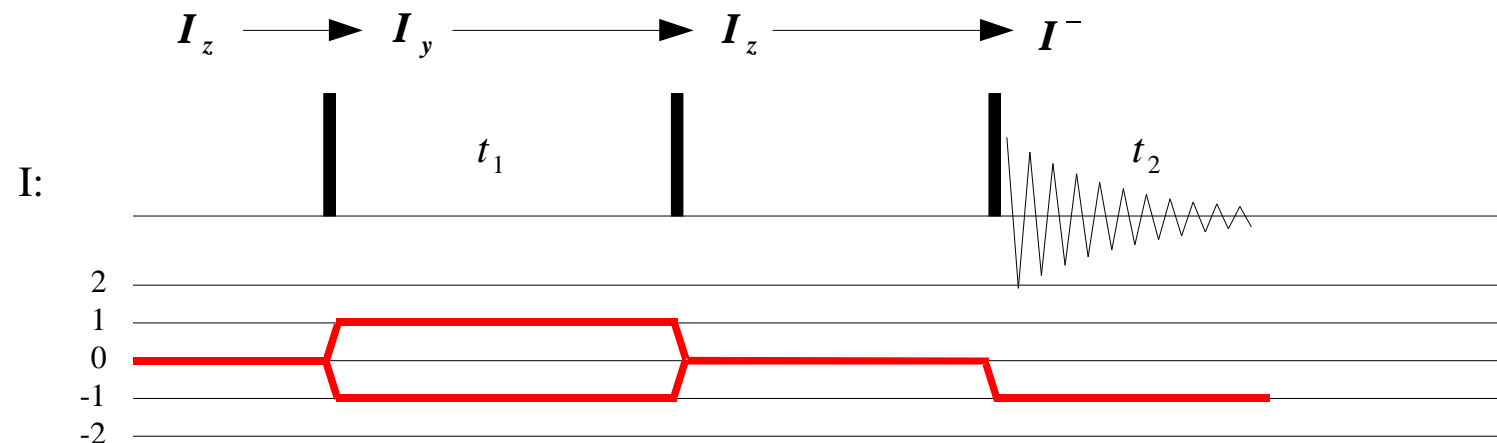
Coherences in NMR (transversal magnetization) can be classified by their coherence order p , this is the number of I^+ operators (positive coherence), and I^- operators (negative coherence)

example:	$I_x = \frac{1}{2}(I^+ + I^-)$	—————► $p=1$ und $p=-1$
	I_z	—————► $p=0$
	$2I_x S_x = \frac{1}{4}(I^+ + I^-)(S^+ + S^-)$	—————► $p=2$ und $p=0$ und $p=-2$
	$= \frac{1}{4}[I^+ S^+ + I^+ S^- + I^- S^+ + I^- S^-]$	

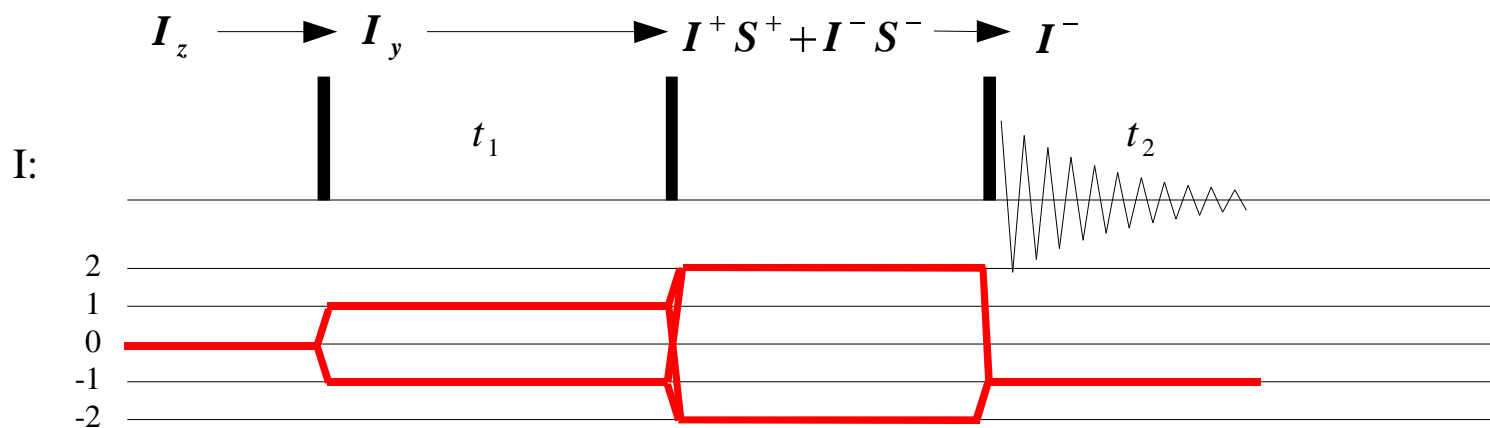
Goal in a (multidimensional) NMR experiment is properly selecting a defined coherence transfer pathway and suppressing all other transfer pathway in order to get an easy interpretable spectrum.

Coherence transfer pathways in homonuclear 3-pulse experiments

A) NOESY

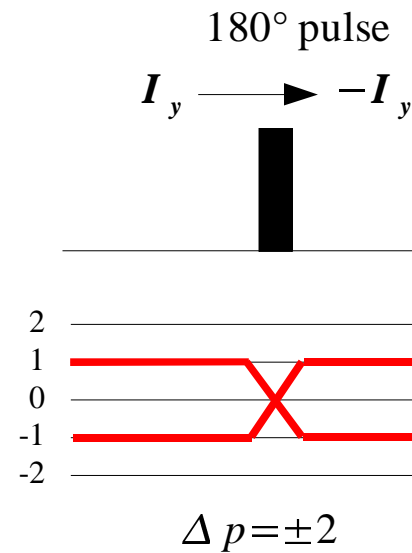
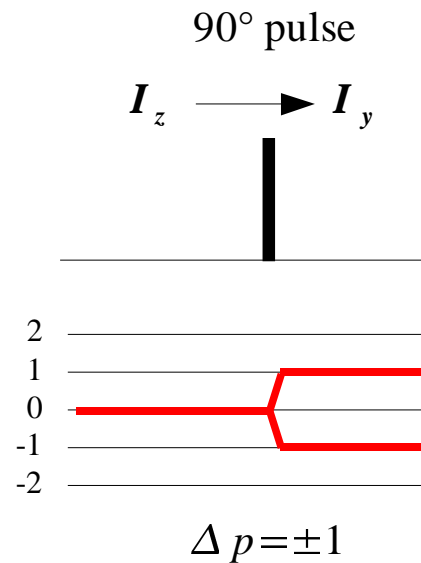


B) DQF-COSY



How can the desired coherence transfer pathway be selected?

1. Pulses change the coherence order



2. Changing the r.f. phase (pulse phase) alters phase of the coherence

$$I_z \xrightarrow{\frac{\pi}{2} I_y} I_x = \frac{1}{2} [I^+ + I^-]$$

$$\Delta \phi_{rf} = \frac{\pi}{2} \quad I_z \xrightarrow{-\frac{\pi}{2} I_x} I_y = -\frac{i}{2} [I^+ + I^-] = \frac{1}{2} [\exp \{-i \frac{\pi}{2}\} I^+ + \exp \{i \frac{\pi}{2}\} I^-]$$

general: a phase alteration of a pulse by $\Delta \phi_{rf}$ results in a phase shift of the coherence with order p by $\Delta \phi = -p \Delta \phi_{rf}$

By systematic variation of the rf-phases together with the receiver phase (phase cycling) in subsequent single experiments it is possible to select desired magnetization transfer pathways and suppressing the unwanted transfers by difference spectroscopy.

Example: phase cycling in the DQF-COSY

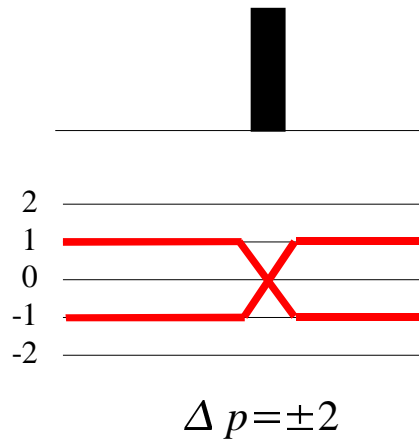
the first both pulses shall create $Dp = \pm 2$ (generation of double quantum coherence)

	ϕ_{rf}	$\phi_{\Delta p=+2}$	$\phi_{\Delta p=-2}$	ϕ_{rec}
x	0°	$0^\circ = 0^\circ$	$0^\circ = 0^\circ$	0°
y	90°	$-180^\circ = 180^\circ$	$180^\circ = 180^\circ$	180°
-x	180°	$-360^\circ = 0^\circ$	$360^\circ = 0^\circ$	0°
-y	270°	$-540^\circ = 180^\circ$	$540^\circ = 180^\circ$	180°

Behaviour of unwanted transfers in this phase cycle:

	ϕ_{rf}	$\phi_{\Delta p=+1}$	$\phi_{\Delta p=-1}$	$\phi_{\Delta p=0}$	ϕ_{rec}
x	0°	$0^\circ = 0^\circ$	$0^\circ = 0^\circ$	$0^\circ = 0^\circ$	0°
y	90°	$-90^\circ = 270^\circ$	$90^\circ = 90^\circ$	$0^\circ = 0^\circ$	180°
-x	180°	$-180^\circ = 180^\circ$	$180^\circ = 180^\circ$	$0^\circ = 0^\circ$	0°
-y	270°	$-270^\circ = 90^\circ$	$270^\circ = 270^\circ$	$0^\circ = 0^\circ$	180°
		↓	↓	↓	
		will be suppressed			

Example: Elimination of imperfections of a 180° refocusing pulse (EXORCYCLE)



$$I^+ \longrightarrow I^+(\Delta p=0) + I^-(\Delta p=-2) + I_z(\Delta p=-1)$$

$$I^- \longrightarrow I^-(\Delta p=0) + I^+(\Delta p=2) + I_z(\Delta p=1)$$

	ϕ_{rf}	$\phi_{\Delta p=+2}$	$\phi_{\Delta p=-2}$	ϕ_{rec}
x	0°	0° = 0°	0° = 0°	0°
y	90°	-180° = 180°	180° = 180°	180°
-x	180°	-360° = 0°	360° = 0°	0°
-y	270°	-540° = 180°	540° = 180°	180°

Behaviour of unwanted transfers in this phase cycle:

	ϕ_{rf}	$\phi_{\Delta p=+1}$	$\phi_{\Delta p=-1}$	$\phi_{\Delta p=0}$	ϕ_{rec}
x	0°	0° = 0°	0° = 0°	0° = 0°	0°
y	90°	-90° = 270°	90° = 90°	0° = 0°	180°
-x	180°	-180° = 180°	180° = 180°	0° = 0°	0°
-y	270°	-270° = 90°	270° = 270°	0° = 0°	180°
		↓	↓	↓	
			will be eliminated		

General aspects of phase cycles

The minimal phase cycle determines the necessary number of scans per t_1 -increment

With many pulses it is no more practicable to alter all rf-phases independently, because the number of required accumulations will increase the overall experimental time.

It is not nice if the necessary number of accumulations for phase cycle is larger than required for a given sample concentration. In this case the experimental time is longer than necessary for generating sufficient intensity.

Phase cycles act as difference methods. If a very intense signal must be eliminated by phase cycling, instabilities cause a non perfect suppression of these signal, because of small signal intensity variations in subsequent scans.

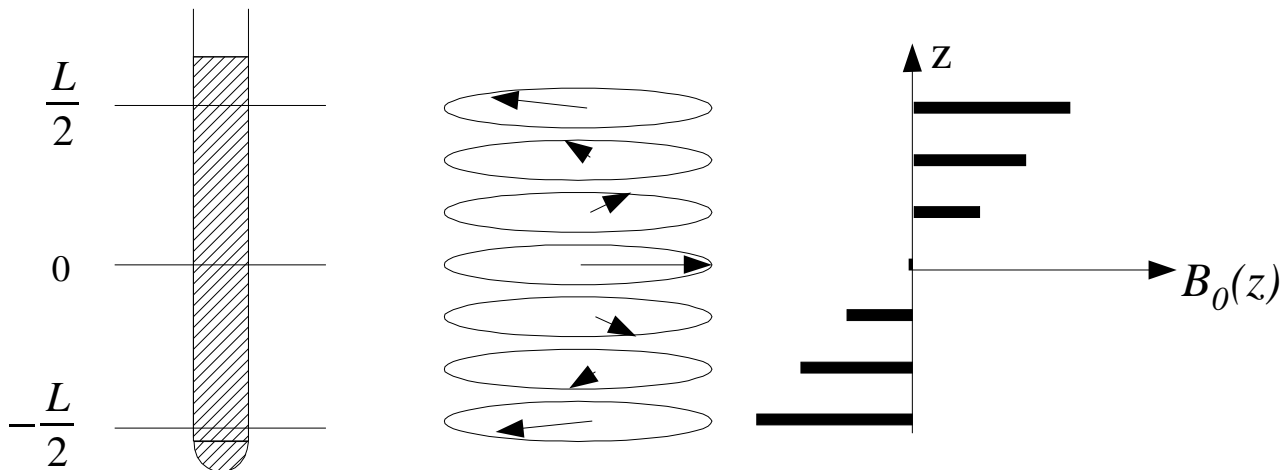
Pulsed field gradients

pulsed field gradients are short (pulse duration: 0.1- 2 ms) defined variations of the external static B_0 field, causing defined spatial inhomogeneities during these gradient pulses.

$$B_0(z) = B_0 + z \frac{\Delta B}{\Delta z}$$

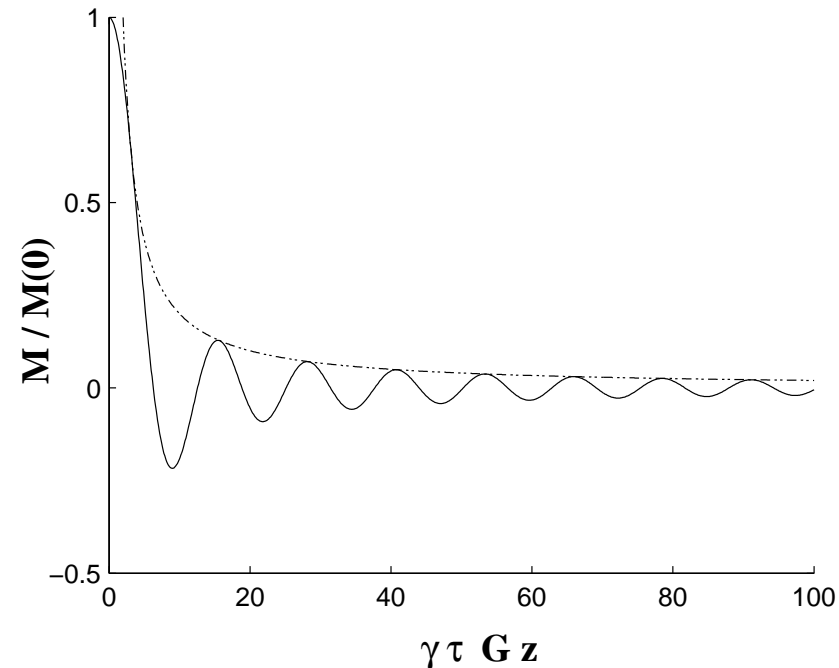
- resonance frequency depends on spatial position: $\omega_0(z) = -\gamma B_0(z) = -\gamma B_0 - \gamma z G_z$
- After the gradient pulse the coherences have acquired a spatial depending phase:

$$\begin{aligned} I^+ &\xrightarrow{\omega_0(z)\tau_{grd}I_z} I^+ \exp\{i z G_z \tau_{grd}\} = I^+ \exp\{i \phi_{grd}(z)\} & \text{with } \phi_{grd}(z) = \gamma z G_z \tau_{grd} \\ I^- &\xrightarrow{\omega_0(z)\tau_{grd}I_z} I^- \exp\{-i z G_z \tau_{grd}\} = I^- \exp\{-i \phi_{grd}(z)\} \end{aligned}$$



The macroscopic observable signal is given by the integrated signal intensity over the sample volume:

$$\begin{aligned}
 I^+(\tau_{grd}) &= \frac{1}{L} I^+(0) \int_{-\frac{L}{2}}^{\frac{L}{2}} \exp \{i \gamma G_z \tau_{grd} z\} dz \\
 &= I^+(0) \frac{\sin(\gamma G_z \tau_{grd} L/2)}{\gamma G_z \tau_{grd} L/2} = I^+(0) \text{sinc}(\gamma G_z \tau_{grd} L/2)
 \end{aligned}$$



For sufficient long gradient pulses the decay of macroscopic observed coherence due to dephasing by the gradient is given by $2/(\gamma G_z L \tau_{grd})$

With a sample length of 4 cm and a typical gradient strength of 10 Gauss / cm the macroscopic observable coherence is reduced to less than 0.2 % with a 1 ms gradient pulse .

—————► transverse magnetization can be dephased very efficiently by pulsed field gradients.

Behaviour of mixed product operators under action of pulsed field gradients

$$I^+ S_z \xrightarrow{\gamma_I z G_z \tau_{grd} I_z} I^+ S_z \exp \{i \gamma_I z G_z \tau_{grd}\} = I^+ S_z \exp \{i \phi_{grd}^I(z)\}$$

$$I^+ S^+ \xrightarrow{\gamma_I z G_z \tau_{grd} I_z} \xrightarrow{\gamma_S z G_z \tau_{grd} S_z} I^+ S^+ \exp \{i \gamma_I z G_z \tau_{grd}\} \exp \{i \gamma_S z G_z \tau_{grd}\} \\ = I^+ S^+ \exp \{i(\phi_{grd}^I(z) + \phi_{grd}^S(z))\}$$

$$I^+ S^- \xrightarrow{\gamma_I z G_z \tau_{grd} I_z} \xrightarrow{\gamma_S z G_z \tau_{grd} S_z} I^+ S^- \exp \{i \gamma_I z G_z \tau_{grd}\} \exp \{-i \gamma_S z G_z \tau_{grd}\} \\ = I^+ S^- \exp \{i(\phi_{grd}^I(z) - \phi_{grd}^S(z))\}$$

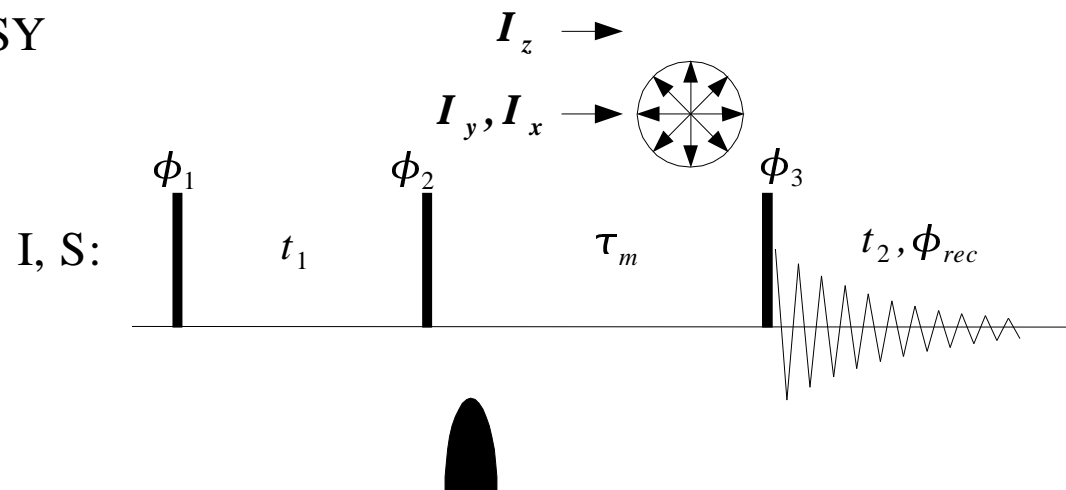
—————► The resulting spatial dependent phase depends linear on the coherence order

$$\phi_{grd}(z) = p \gamma z G_z \tau_{grd}$$

—————► pulsed field gradients allow the discrimination of different coherences within a single scan !!

Dephasing of undesired transverse magnetization with pulsed field gradients

NOESY



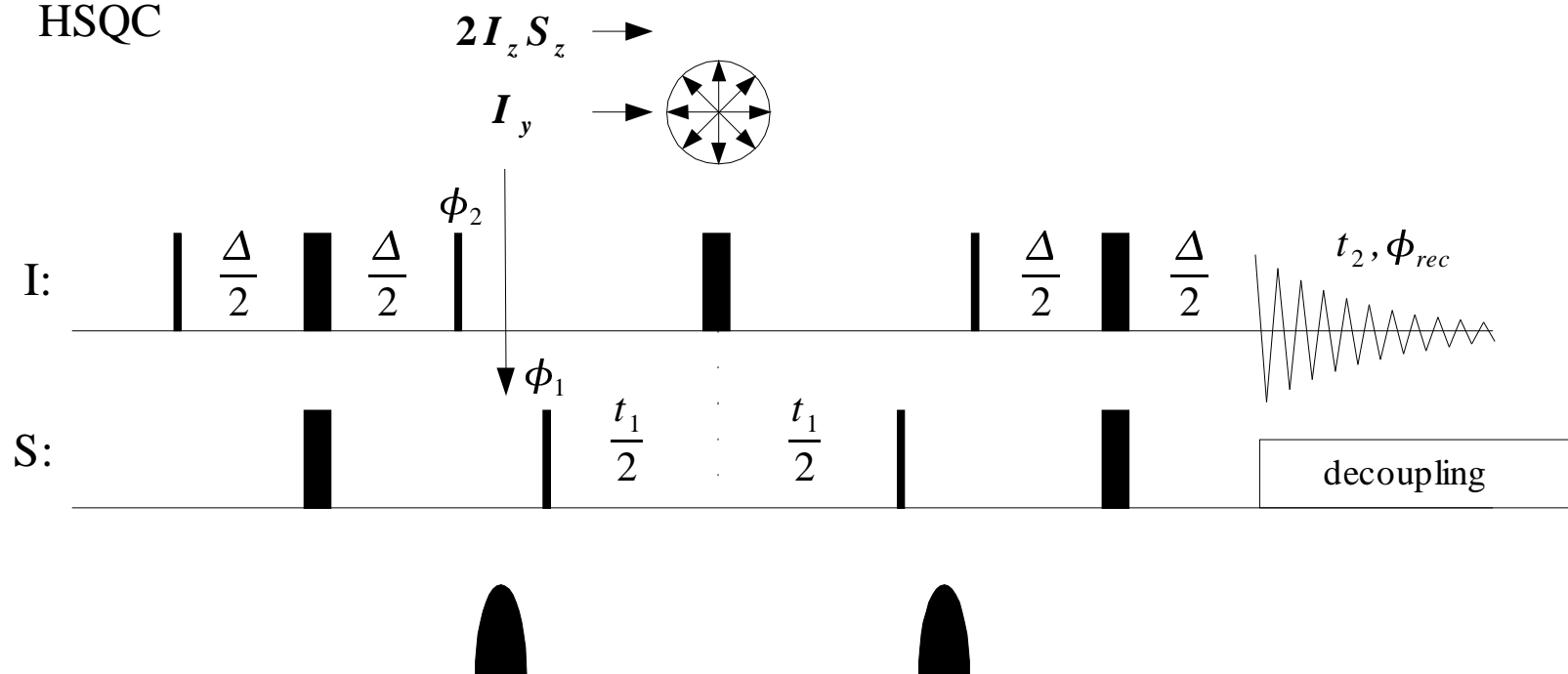
$$\phi_1 = (x, -x) + SHR$$

$$\phi_2 = (x, x, -x, -x)$$

$$\phi_3 = (x, x, x, x, -x, -x, -x, -x)$$

$$\phi_{rec} = (x, -x, x, -x, -x, x, x, -x)$$

HSQC



$$\Delta \approx \frac{1}{2J_{IS}}$$

$$\phi_1 = \{x, -x\} + SHR$$

$$\phi_2 = \{y, y, -y, -y\}$$

$$\phi_{rec} = \{x, -x, -x, x\}$$

Defined de- and rephasing with pulsed field gradients

If a desired coherence (transverse magnetization) is dephased by a pulsed field gradient, a second gradient must rephase the spatial variation along the sample in order to get an observable signal:

example:

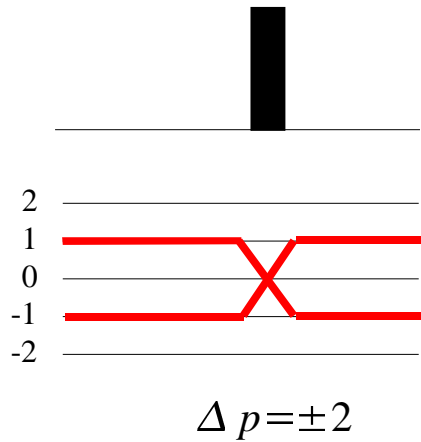
$$I^+ \xrightarrow{G_A(z)} I^+ \exp\{i\phi_A(z)\} \quad \text{---} \quad \text{---} \quad \xrightarrow{G_B(z)} I^+ \exp\{i\phi_A(z)\} \exp\{i\phi_B(z)\}$$

to achieve a macroscopic observable signal, the second gradient must compensate the dephasing caused by the first gradient:

$$\exp\{i\phi_A(z)\} \exp\{i\phi_B(z)\} = \exp\{i(\phi_A(z) + \phi_B(z))\} = 1 \quad \text{that means } \phi_A(z) + \phi_B(z) = 0$$

—► By setting strength and duration of different gradients defined selections of coherence transfer pathways within a single scan are possible

Selection of refocusing within a single scan by a pulsed field gradient

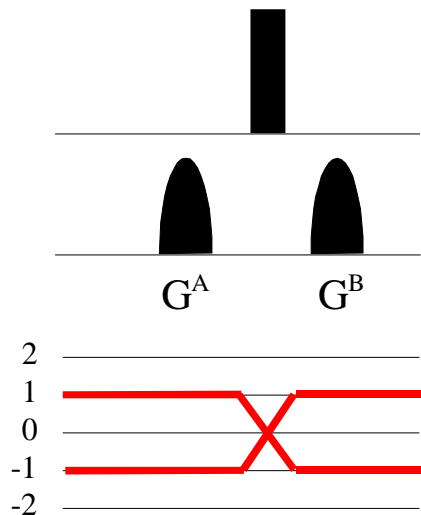


$$I^+ \longrightarrow I^+(\Delta p=0) + I^-(\Delta p=-2) + I_z(\Delta p=-1)$$

$$I^- \longrightarrow I^-(\Delta p=0) + I^+(\Delta p=2) + I_z(\Delta p=1)$$

Suppression of undesired transfers by phase cycling \longrightarrow EXORCYCLE

\longrightarrow four independent scans necessary

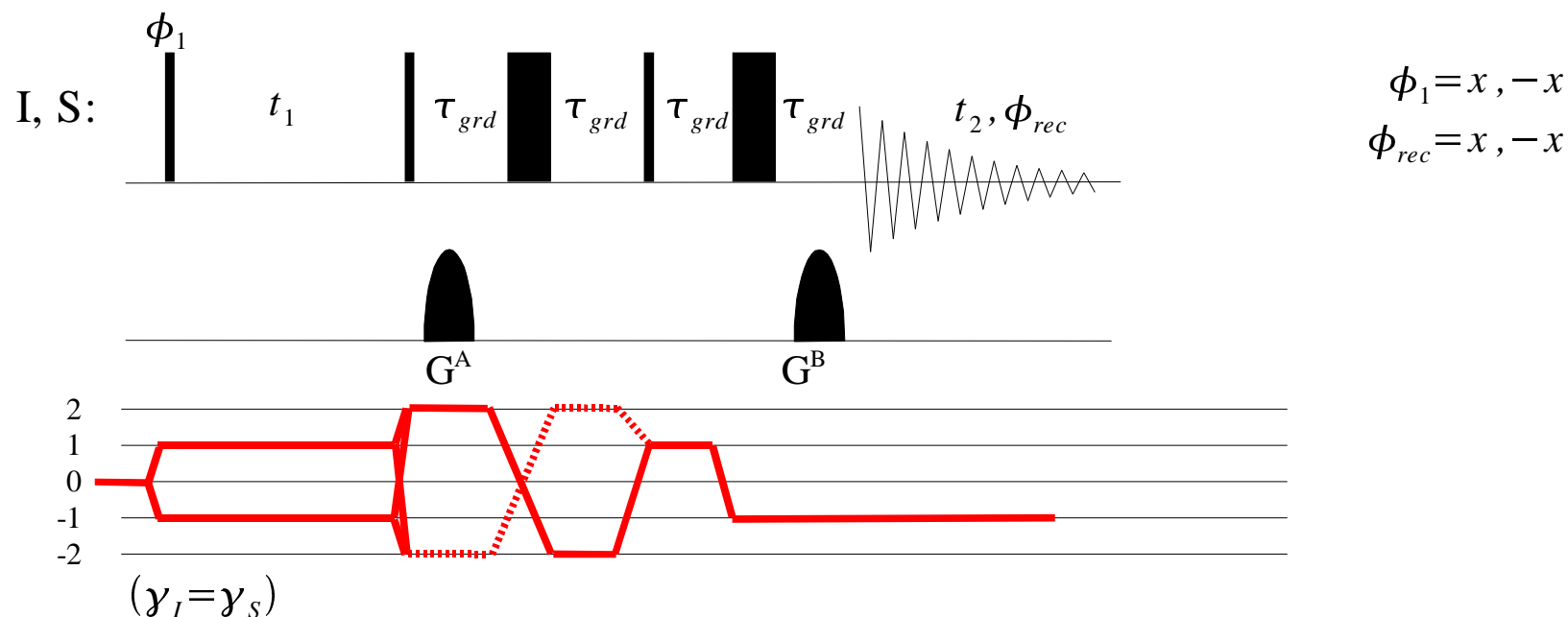


$$I^+ \longrightarrow I^+ \exp \{i(\phi_{grd}^A + \phi_{grd}^B)\} + I^- \exp \{i(\phi_{grd}^A - \phi_{grd}^B)\} + I_z \exp \{i\phi_{grd}^A\}$$

$$I^- \longrightarrow I^- \exp \{-i(\phi_{grd}^A + \phi_{grd}^B)\} + I^+ \exp \{-i(\phi_{grd}^A - \phi_{grd}^B)\} + I_z \exp \{-i\phi_{grd}^A\}$$

\longrightarrow $G^A = G^B$ selects the refocusing within a single scan and suppresses the unwanted transfers

Coherence selection in the DQF-COSY by pulsed field gradients



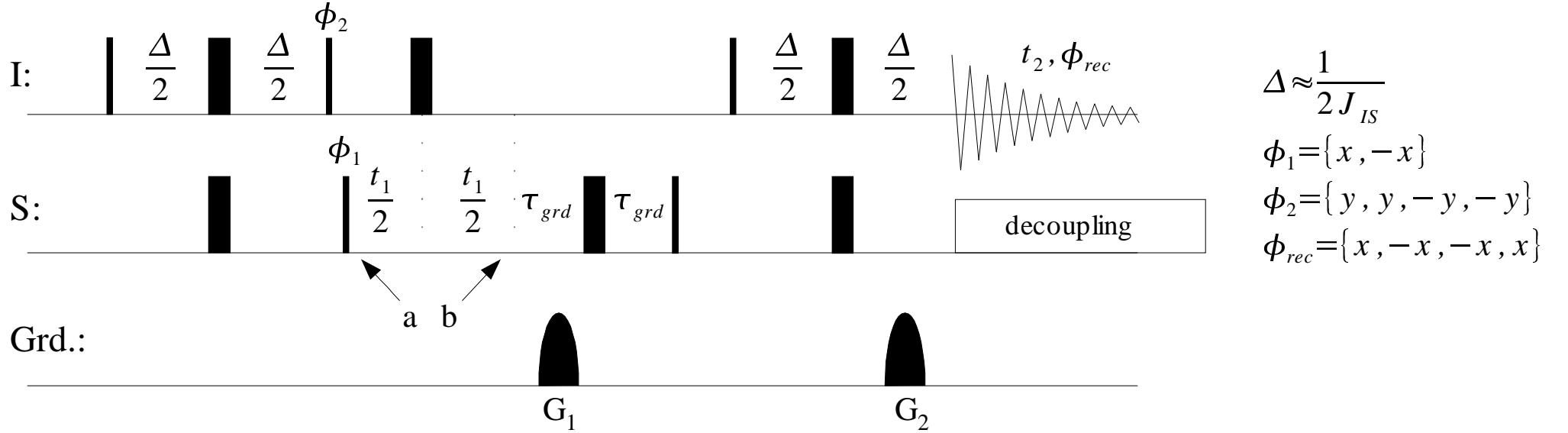
$$2I^+ S^+ \exp\{i 2\phi_{grd}^A(z)\} \longrightarrow I^- \exp\{i(2\phi_{grd}^A(z) - \phi_{grd}^B(z))\} \quad 2\phi_{grd}^A = \phi_{grd}^B$$

$$2I^- S^- \exp\{-i 2\phi_{grd}^A(z)\} \longrightarrow I^- \exp\{i(-2\phi_{grd}^A(z) - \phi_{grd}^B(z))\} \quad -2\phi_{grd}^A = \phi_{grd}^B$$

→ Only the transfer $2I^+ S^+ \rightarrow I^-$ or the transfer $2I^- S^- \rightarrow I^-$ can be selected in a single scan, but not both !

The spinecho $\tau_{grd} - 180^\circ - \tau_{grd}$ serves for refocusing of the evolution of chemical shifts during the duration of the gradient (avoids a large first order phase error)

Coherence selection in the HSQC by pulsed field gradients



$$\sigma(a) = -2I_z S_y = i[I_z S^+ - I_z S^-] \longrightarrow \sigma(b) = -i[I_z S^+ \exp\{-i\Omega_s t_1\} - I_z S^- \{i\Omega_s t_1\}]$$

$$\xrightarrow{G_1} \sigma(b) = -i[I_z S^+ \exp\{-i(\Omega_s t_1 - \phi_1(z))\} - I_z S^- \{i(\Omega_s t_1 - \phi_1(z))\}] \quad \text{mit} \quad \phi_1(z) = \gamma_s \tau_{grd} G_1 z$$

$$\xrightarrow{\pi S_x} \frac{1}{2}[-i2I_z S_x - 2I_z S_y] \exp\{-i(\Omega_s t_1 - \phi_1(z))\} + \frac{1}{2}[i2I_z S_x - 2I_z S_y] \exp\{i(\Omega_s t_1 - \phi_1(z))\} \quad 2I_z S_x \rightarrow N.O.T.$$

$$\begin{aligned} \longrightarrow \frac{1}{2}[(-\frac{1}{2})I^-] \exp\{-i(\Omega_s t_1 - \phi_1(z))\} & \longrightarrow \frac{1}{2}[(-\frac{1}{2})I^-] \exp\{-i\Omega_s t_1\} \exp\{i\Omega_I t_2\} \exp\{i(\phi_1(z) - \phi_2(z))\} \\ + \frac{1}{2}[(-\frac{1}{2})I^-] \exp\{i(\Omega_s t_1 - \phi_1(z))\} & + \frac{1}{2}[(-\frac{1}{2})I^-] \exp\{i\Omega_s t_1\} \exp\{i\Omega_I t_2\} \exp\{-i(\phi_1(z) + \phi_2(z))\} \end{aligned}$$

in order to obtain a macroscopic observable signal the spatial dependent phases caused by the two gradients must be cancel each other:

$$\phi_1(z) = \phi_2(z)$$



selection of transfer

$$I_z S^+ \rightarrow \frac{1}{4} I^-$$

$$\gamma_S \tau_{grd} G_1 z = \gamma_I \tau_{grd} G_2 z$$

$$\frac{G_1}{G_2} = \frac{\gamma_I}{\gamma_S}$$

under the assumption that the duration of both gradients are equal

or

$$-\phi_1(z) = \phi_2(z)$$



selection of transfers

$$I_z S^- \rightarrow \frac{1}{4} I^-$$

$$-\gamma_S \tau_{grd} G_1 z = \gamma_I \tau_{grd} G_2 z$$

$$-\frac{G_1}{G_2} = \frac{\gamma_I}{\gamma_S}$$

under the assumption that the duration of both gradients are equal

In both cases a phasemodulated signal results:

$$Signal(t_1, t_2) = \frac{1}{4} \exp \{-i \Omega_S t_1\} \exp \{i \Omega_I t_2\} \quad \text{mit} \quad \gamma_S G_1 = \gamma_I G_2$$

$$Signal(t_1, t_2) = \frac{1}{4} \exp \{i \Omega_S t_1\} \exp \{i \Omega_I t_2\} \quad \text{mit} \quad \gamma_S G_1 = -\gamma_I G_2$$

With the alternation of the polarity (sign) of G1 (or G2) for a given t_1 inkrement a phasele hypercomplex signal can be created by linear combination:

$$Signal_N(t_1, t_2) = \frac{1}{4} \exp \{-i \Omega_S t_1\} \exp \{i \Omega_I t_2\} \quad \text{mit} \quad \gamma_S G_1 = \gamma_I G_2$$

$$Signal_P(t_1, t_2) = \frac{1}{4} \exp \{i \Omega_S t_1\} \exp \{i \Omega_I t_2\} \quad \text{mit} \quad \gamma_S G_1 = -\gamma_I G_2$$

$$\longrightarrow \quad Signal_{\cos}(t_1, t_2) = Signal_P(t_1, t_2) + Signal_N(t_1, t_2) = \frac{1}{2} \cos(\Omega_S t_1) \exp \{i \Omega_I t_2\}$$

$$Signal_{\sin}(t_1, t_2) = i(Signal_P(t_1, t_2) - Signal_N(t_1, t_2)) = \frac{1}{2} \sin(\Omega_S t_1) \exp \{i \Omega_I t_2\}$$

„echo-antiecho transformation“

After the echo-antiecho transformation the resulting twodimensional FID shows the same signal intensity like a 'classical' HSQC, recorded phase sensitive by the SHR method,

but

during the echo-antiecho transformation the noise from both single experiments adds up, and for the noise level results::

$$|Noise_{\cos, \sin}| = |Noise_P + Noise_N| = \sqrt{2} |Noise_P| \quad \longrightarrow \quad S/N(SHR) = \sqrt{2} S/N(grd. selection)$$

Comparing the two coherence selections with gradients in the experiment HSQC and DQF COSY the following aspects result:

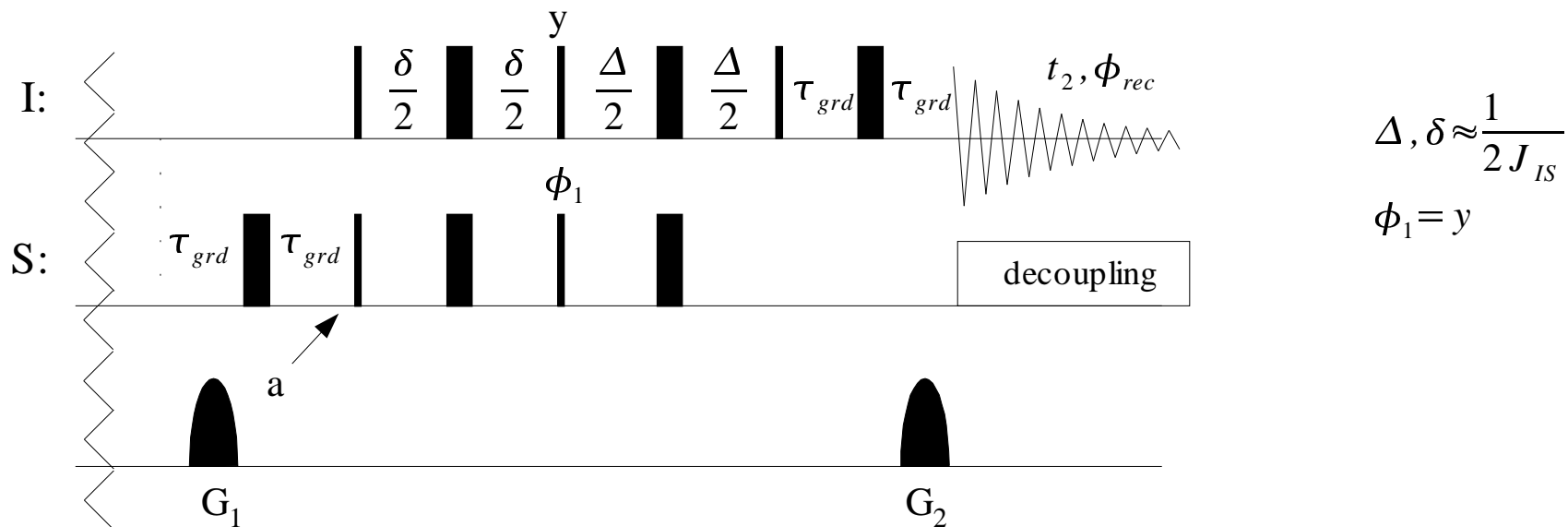
1. Selection by gradients during a fixed time interval (e.g. in the DQF-COSY) reduces the signal intensity by a factor of 2 compared to the selection with a proper phase cycling, because only the positive or the negative coherence results in observable signal.
2. Selection by a gradient during the evolution period reduces the overall signal intensity to $\frac{1}{\sqrt{2}} \text{signal}(\text{phase cycling})$, if only one of both cartesian components of the desired coherence is transferred to the final observed signal.

The question now is, whether the transfer

$$I_z S^+ = \frac{1}{2} [2I_z S_x + i 2I_z S_y] \rightarrow \frac{1}{2} I^-$$

is possible, that both cartesian components can be transferred to the observable signal.

Coherence order selective transfer (sensitivity enhancement)



$$\sigma(a) = \frac{1}{2} [-i 2I_z S_x - 2I_z S_y] \exp \{-i(\Omega_S t_1 - \phi_1(z))\} \\ + \frac{1}{2} [i 2I_z S_x - 2I_z S_y] \exp \{i(\Omega_S t_1 - \phi_1(z))\}$$

Transformation of both cartesian components (relevant interactions only):

$$\begin{array}{ccccccccccc} 2I_z S_y & \xrightarrow{\frac{\pi}{2}(I_x + S_x)} & -2I_y S_z & \xrightarrow{\delta \pi J 2I_z S_z} & I_x & \xrightarrow{\frac{\pi}{2} I_y} & -I_z & \xrightarrow{\pi I_x} & I_z & \xrightarrow{\frac{\pi}{2} I_x} & -I_y & \xrightarrow{\pi I_x} & I_y \\ 2I_z S_x & \xrightarrow{\frac{\pi}{2}(I_x + S_x)} & 2I_y S_x & \xrightarrow{\pi I_x} & 2I_y S_x & \xrightarrow{\frac{\pi}{2}(I_y + S_y)} & -2I_y S_z & \xrightarrow{\Delta \pi J 2I_z S_z} & I_x \end{array}$$

the overall transfer with these transformation is given by:

$$\begin{aligned} \frac{1}{2}[-i2\mathbf{I}_z\mathbf{S}_x-2\mathbf{I}_z\mathbf{S}_y] &\longrightarrow \frac{1}{2}[(-i)\mathbf{I}_x-\mathbf{I}_y]=\frac{(-i)}{2}\mathbf{I}^- \\ +\frac{1}{2}[i2\mathbf{I}_z\mathbf{S}_x-2\mathbf{I}_z\mathbf{S}_y] &\qquad\qquad +\frac{1}{2}[i\mathbf{I}_x-\mathbf{I}_y]=\frac{i}{2}\mathbf{I}^+ \end{aligned}$$

with relative gradient strengths $\gamma_S G_1 = \gamma_I G_2$ the transfer $\mathbf{I}_z\mathbf{S}^+ \rightarrow \frac{1}{2}\mathbf{I}^-$ is selected.

This results in the following observed signal: $Signal_N(t_1, t_2) = \frac{1}{2} \exp\{-i\Omega_S t_1\} \exp\{i\Omega_I t_2\}$

With the gradient strengths $\gamma_S G_1 = -\gamma_I G_2$ and $\phi_1 = -$ the transfer $\mathbf{I}_z\mathbf{S}^- \rightarrow \frac{1}{2}\mathbf{I}^-$ is selected.

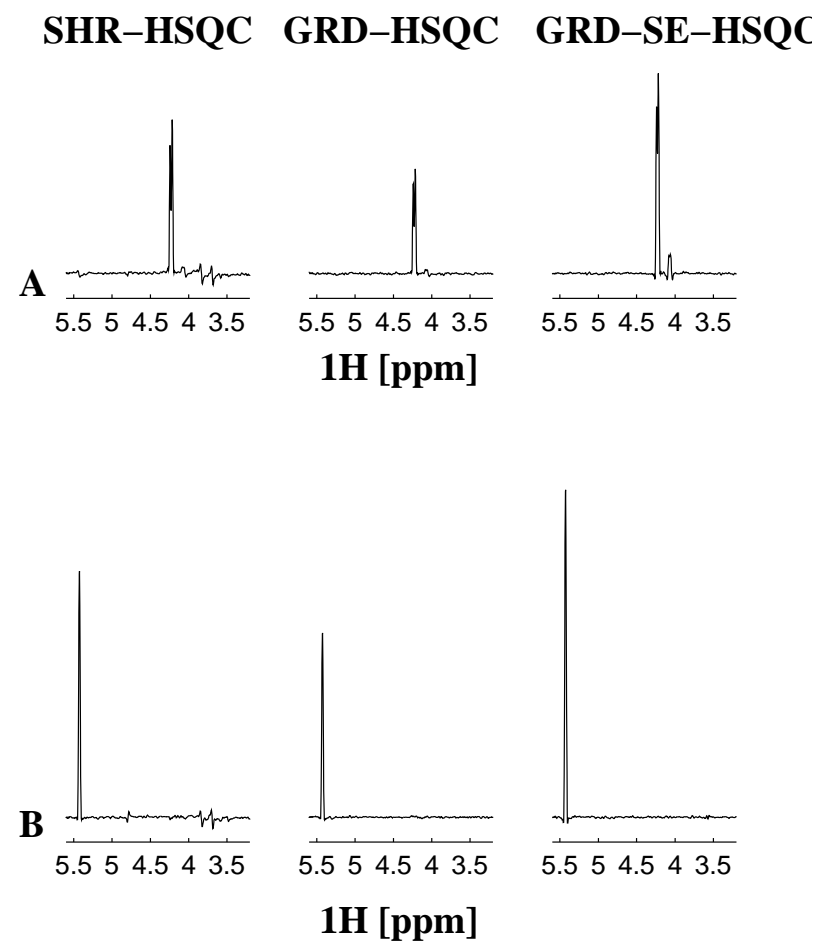
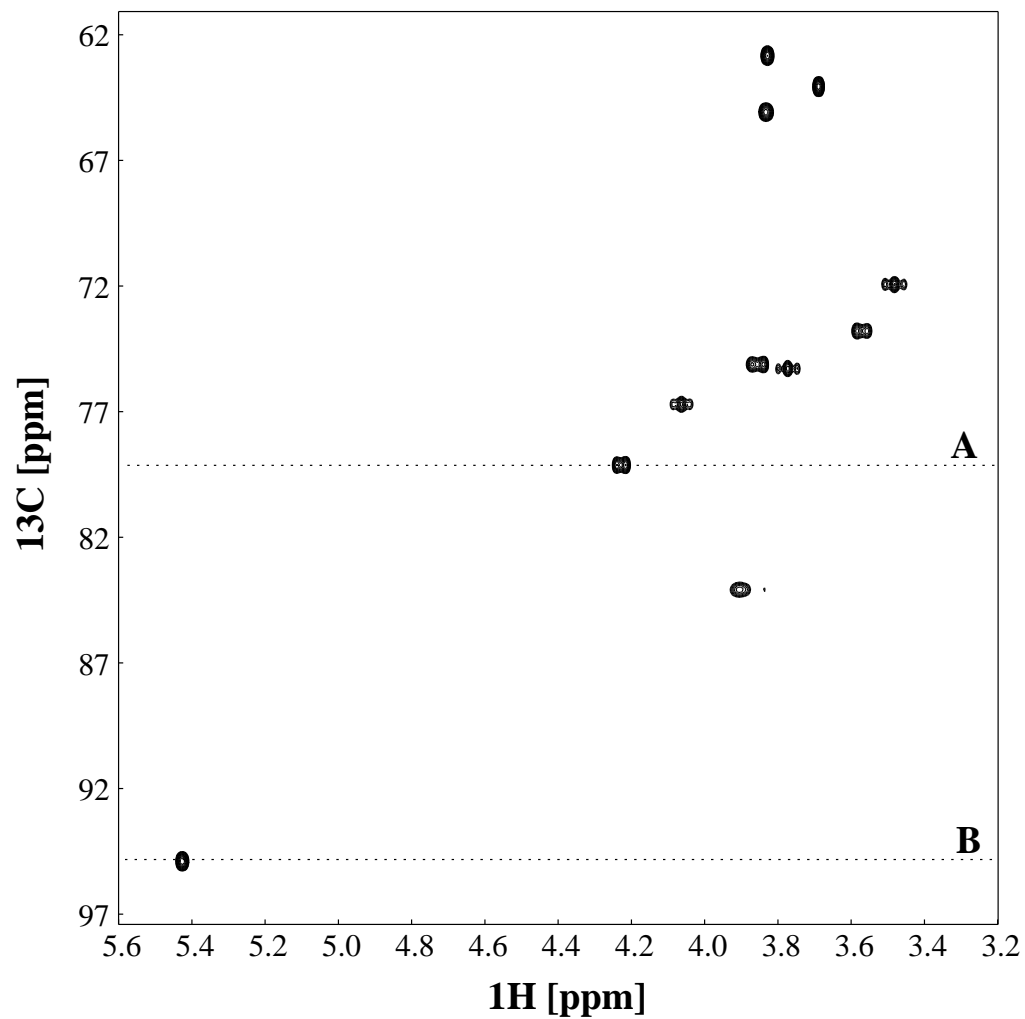
This results in the following observed signal: $Signal_P(t_1, t_2) = \frac{1}{2} \exp\{i\Omega_S t_1\} \exp\{i\Omega_I t_2\}$

The echo-antiecho transformation gives the final twodimensional phase sensitive signal.

This signal intensity is 2 times more intensive compared to the previous selection by gradients, if the additional pulses (imperfections !) and time intervals (relaxation !) cause no further signal loss.

Comparison of different techniques : ^1H , ^{13}C HSQC on sucrose

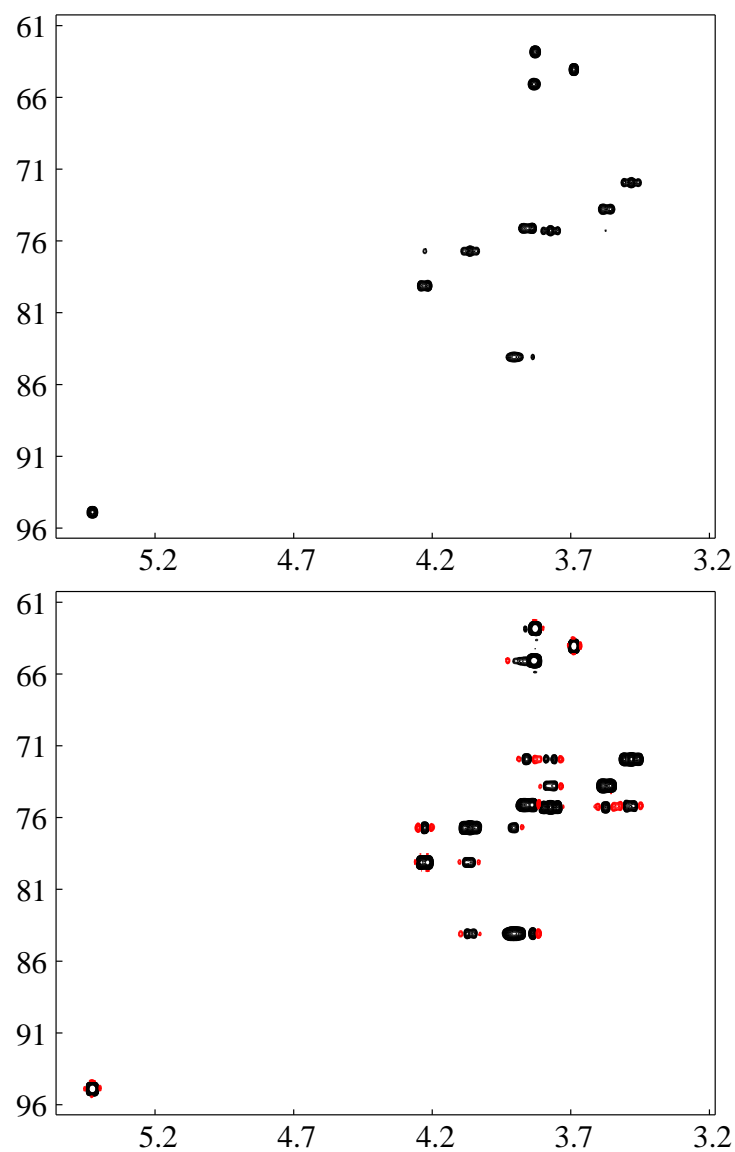
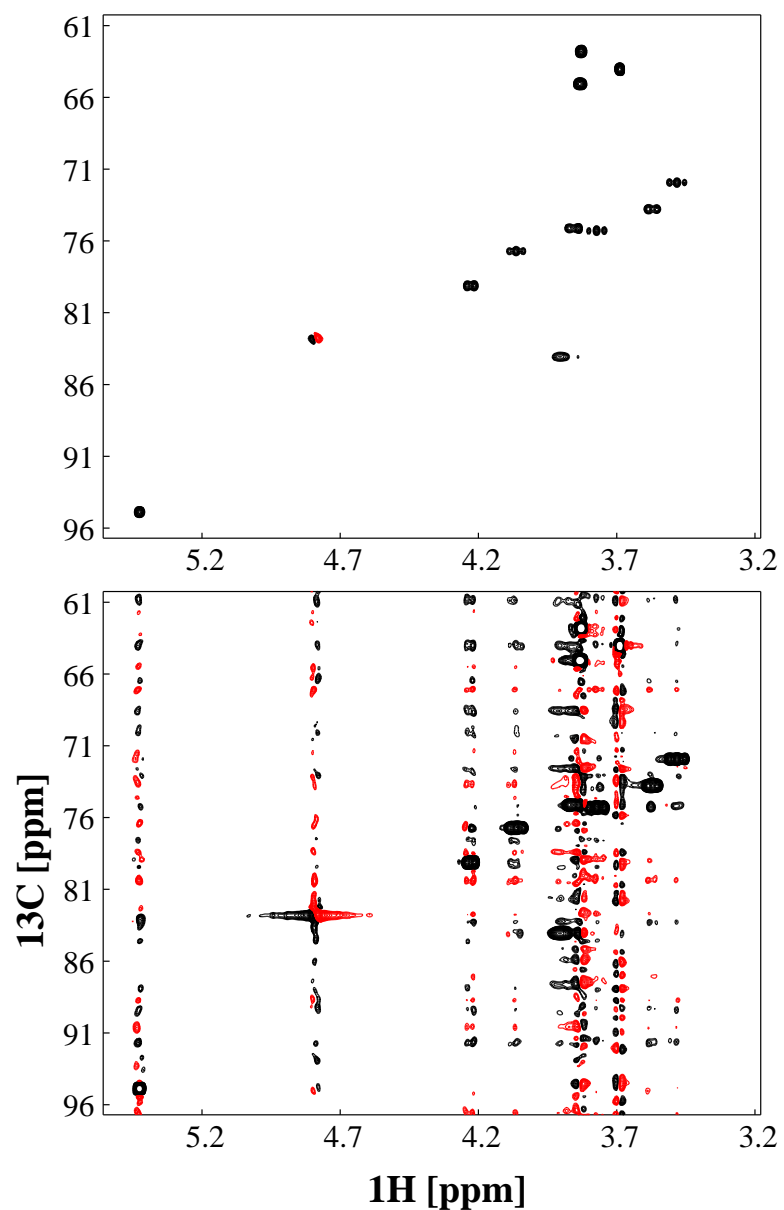
(ca. 15 mM sucrose in D_2O , 400 MHz, 128* (F1) 1024* (F2) data points, NS = 16, total duration ca 1.5 each spectrum)



Artifact elimination using gradient selection

Standard-HSQC

HSQC mit Gradientenselektion



hoher Konturlevel

tiefer Konturlevel

—————▶ **deutliches t1-Rauschen**

—————▶ **t1-Rauschen eliminiert**

Origins of the t_1 -noise

In the chosen pulse program for the standard HSQC the rf phases allow that the resonances from protons not bound to a ^{13}C -spin (natural abundance ^{13}C ca. 99% !!) result in observable signal in the FID.

————▶ These must be suppressed in a difference manner by a proper phase cycling !

Instabilities of the spectrometer causes a not perfect reproducible signal in different scans, therefore along t_1 a variation (noise) of the not perfectly suppressed signal results

In the gradient experiment the signals from protons not bound to ^{13}C -spins are suppressed effective in each single scan. This minimizes the residual t_1 -noise to a large extend.

Water suppression in protein NMR spectroscopy

16-bit analog to digital converter: intensity is measured in integer numbers ranging from -2^8 bis $+2^8-1$, that is from -32768 bis + 32767

proton concentration of H_2O 2 x 55 mol/l, $1.1 \times 10^2 \text{ M}$

typical protein concentration 1 - 2 mM

———► H_2O signal is ca. 50000 - 100000 times more intense than an individual protein proton.

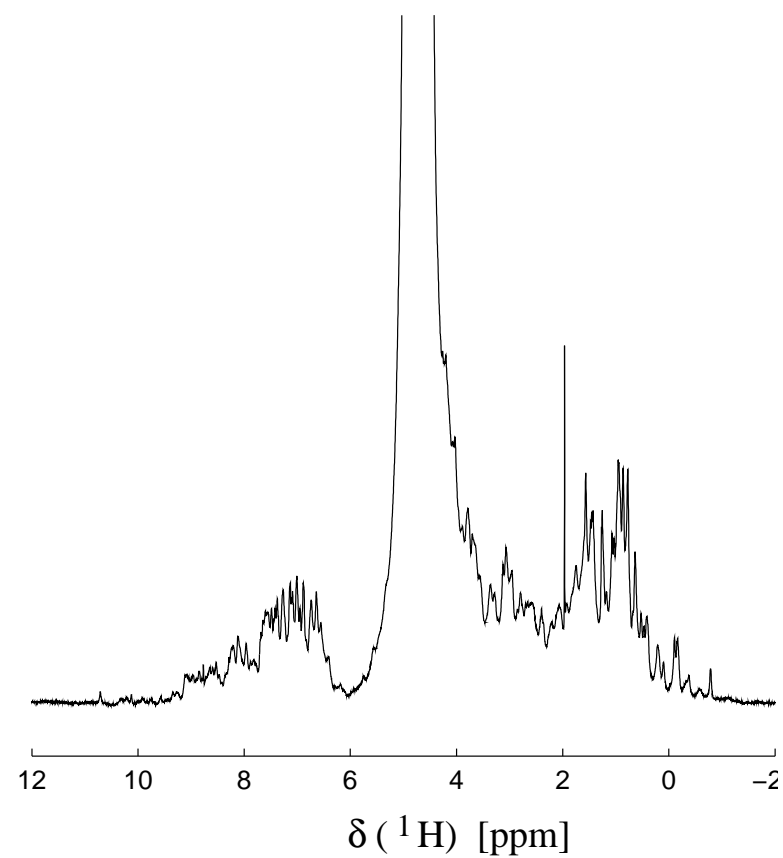
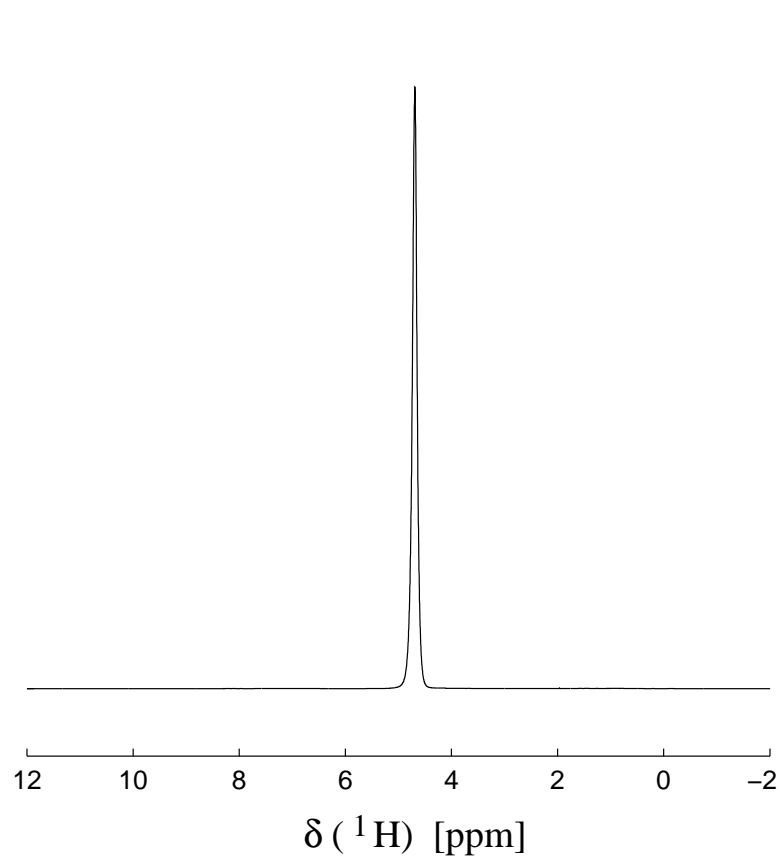
It is often not possible to detect protein signals near the not suppressed water !

———► The essential detection of the amide protons requires samples in H_2O , because in D_2O the exchange of labile protons with deuterons results in their signal loss.

Onedimensional ^1H NMR experiment on protein with out water suppression

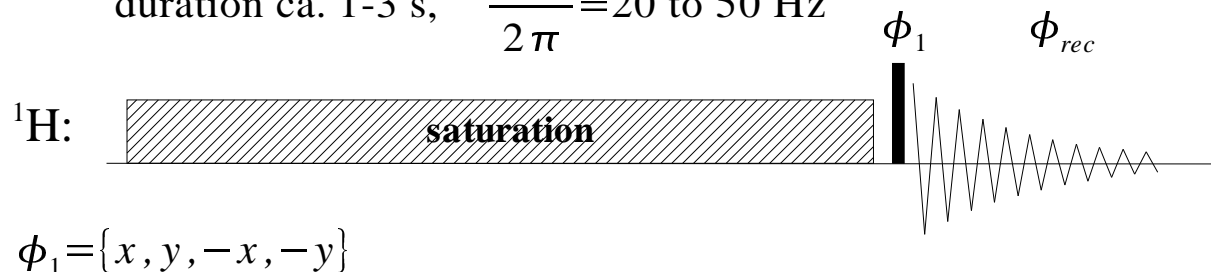
(2 mM lysozyme in 90% H_2O / 10% D_2O , 400 MHz, NS = 32)

600-fache vertikale Expansion

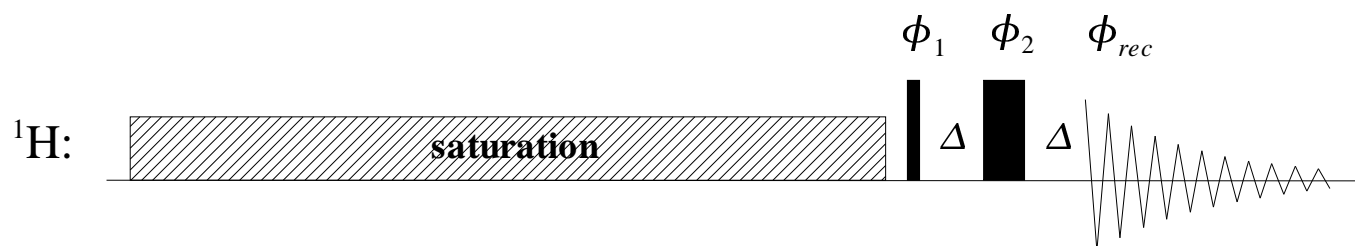


Onedimensional ^1H NMR experiments with presaturation for water suppression

duration ca. 1-3 s, $\frac{\gamma B_1}{2\pi} = 20 \text{ to } 50 \text{ Hz}$



additional spin echo



Δ ca. $100 \mu\text{s}$

$\phi_1 = \{4x, 4y, 4(-x), 4(-y)\}$

$\phi_2 = \{x, y, -x, -y\}$

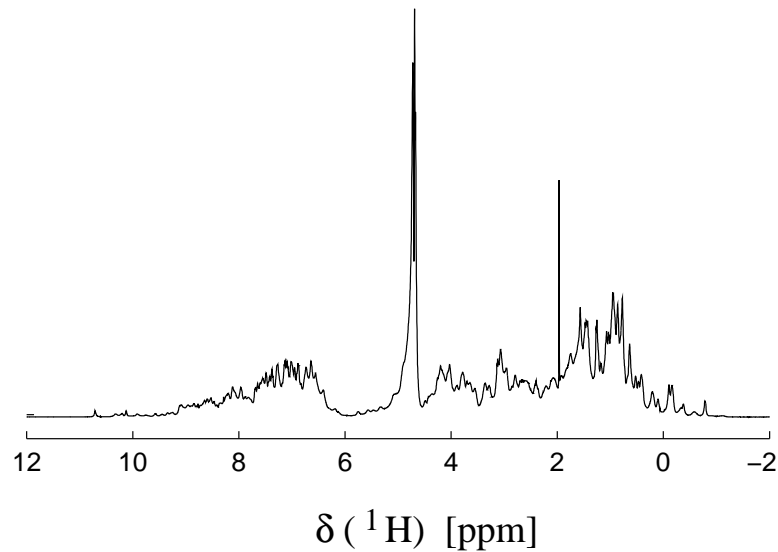
$\phi_{rec} = \{x, -x, x, -x, y, -y, y, -y, -x, -x, -x, -x, -y, y, -y, y\}$

Onedimensional ^1H NMR experimente on a protein in H_2O in water

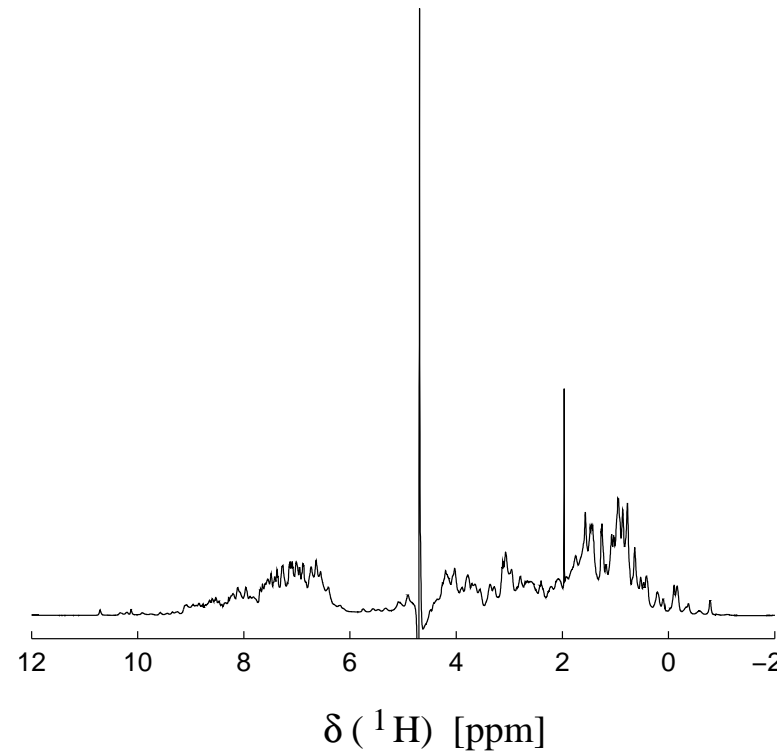
using presaturation for water suppression

(2 mM lysozyme in 90% H_2O / 10% D_2O , 400 MHz, NS = 32, saturation 3 s, $\frac{\gamma B_1}{2\pi} = 49 \text{ Hz}$)

Vorsättigung



Vorsättigung mit Hahn Echo

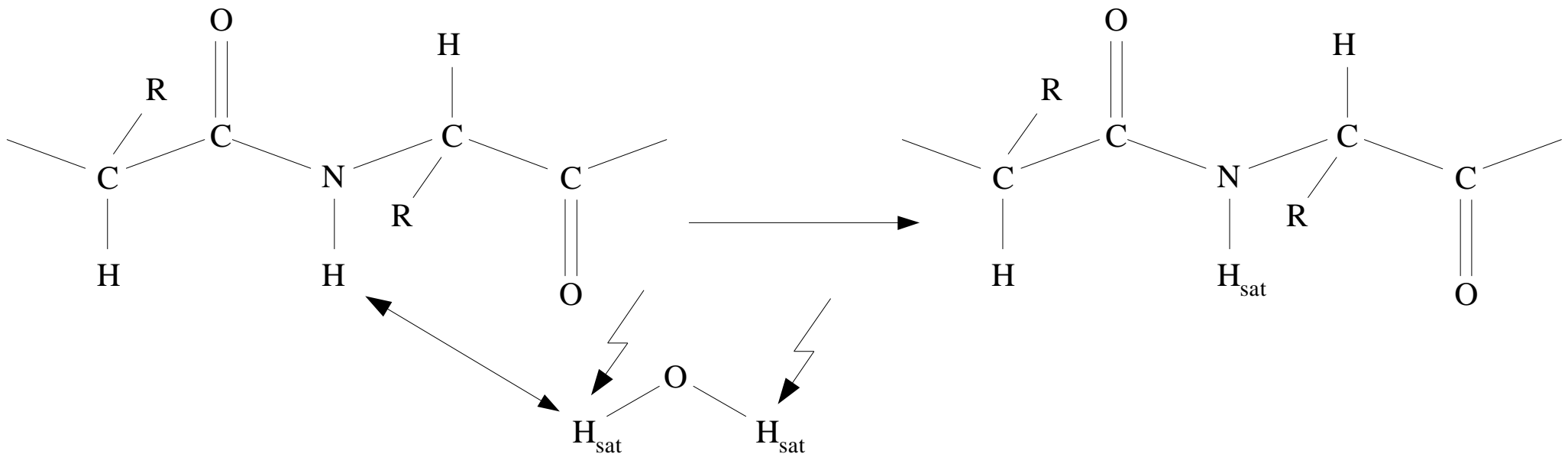


Problems with water suppression by presaturation

Saturation is frequency selective, protein resonances near the water are also saturated

Residual water signal is often most intense signal in the spectrum even after presaturation. In 2D experiments this results in intense t_1 -noise at $F_2 = d(\text{H}_2\text{O})$ and causes baseline distortions.

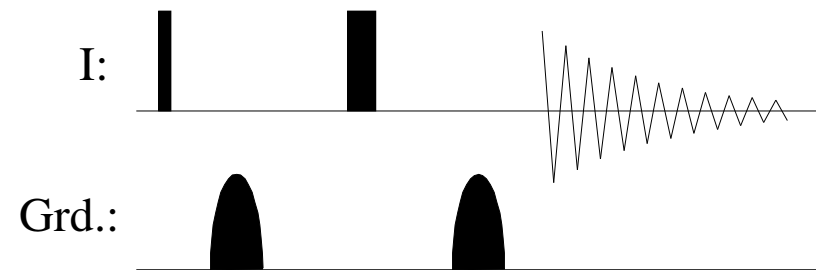
The exchange of labile protons (e.g. amide protons) with water results in saturation transfer, if the exchange rate is faster than the longitudinal relaxation of the exchanging proton



Water suppression with pulsed field gradients

Basic principle: spinecho with two gradients of equal strength and duration

—► good selection of refocusing in a single scan



Goal: The 180° pulse shall only refocus protein magnetization but not the water spins (H_2O antiselective pulse)
in this case the difference of the gradients ($=0$) acts on the protein signals,
and water protons are affected by the sum of the two gradients

—► efficient dephasing of the water magnetization by the gradients

Rotation angle for protein protons: 180°

$$3a(x) - t - 9a(x) - t - 19a(x) - t - 19a(-x) - t - 9a(-x) - t - 3a(-x)$$

$$26a = 180^\circ,$$

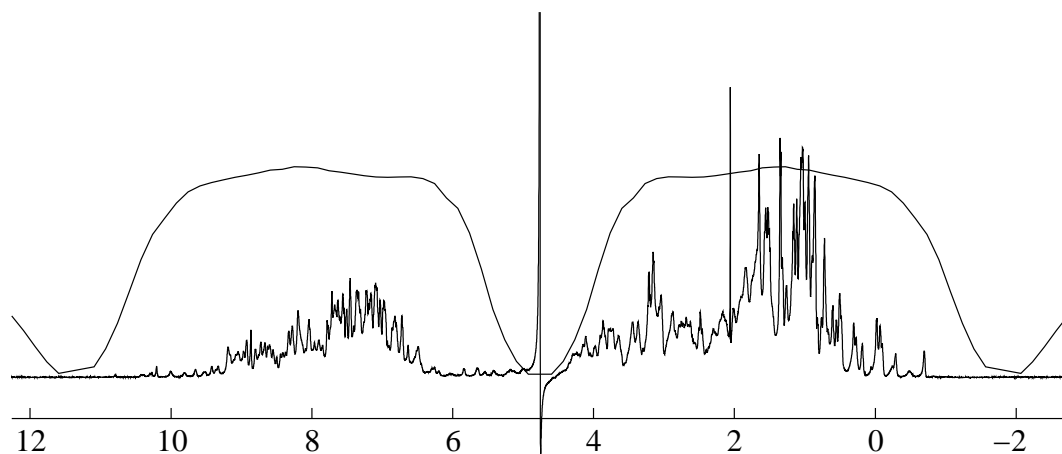
excitation maximum at ca. $1 / (2t)$ relative to carrier frequency

I: 180°(x) 180°(-x)_{H2O} 180°(x) 180°(-x)_{H2O} 180°(x)

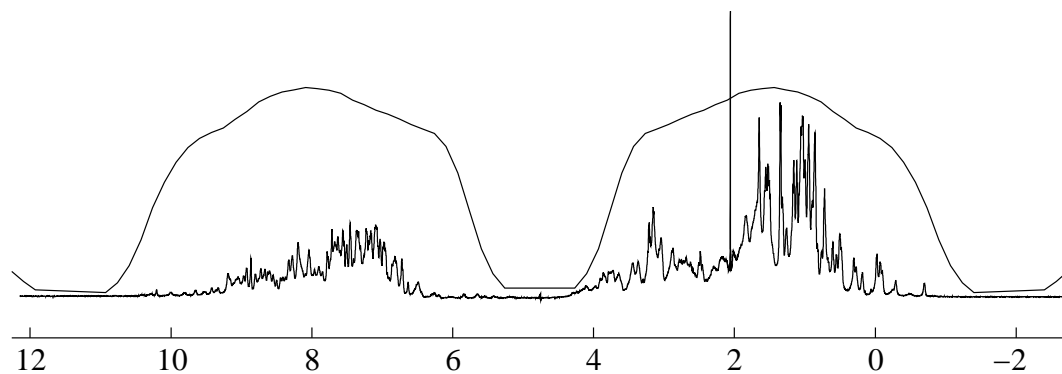
Grd.: G1 G1 G2 G2

Double watergate improves water suppression and compensates the off-resonance effects caused by the first selective pulse.

Binomial (3-9-19) watergate and excitation sculpting on lysozyme in 90 % H₂O / 10 % D₂O

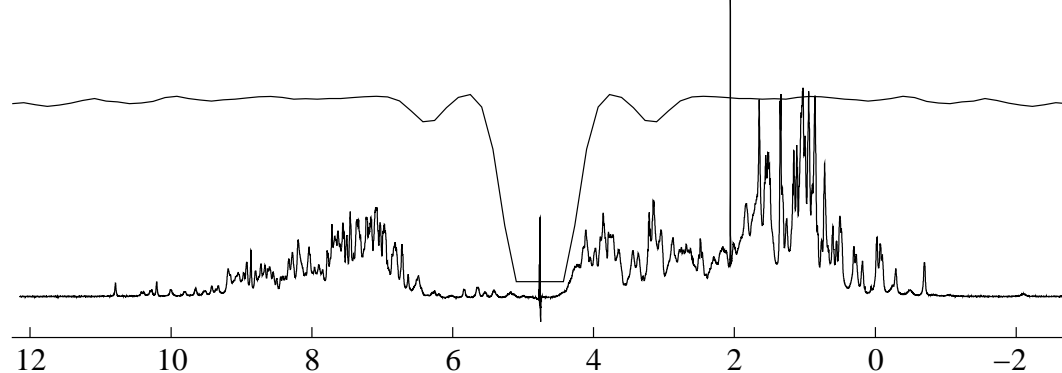


3-9-19 Watergate



3-9-19 Double Watergate

Dauer der Wasserunterdrückung ca. 10 ms



Excitation Sculpting

mit 1.65 ms soft 180° Puls

Dauer der Wasserunterdrückung ca. 10 ms

$\delta (^1\text{H})$ [ppm]

Additional features of watergate-techniques

No continuous saturation during the relaxation delay between the scans

—————▶ reduces saturation and saturation transfer

Water suppression is frequency selective, protons near the water resonance are also affected

The water suppression occurs after the exciting pulse. During the time period necessary for water suppression transverse relaxation reduces the initial signal intensity.

Example: Excitation sculpting, selective pulse 2.5 ms, gradient pulse ca. 0.5 ms

—————▶ total duration ca. 12 ms

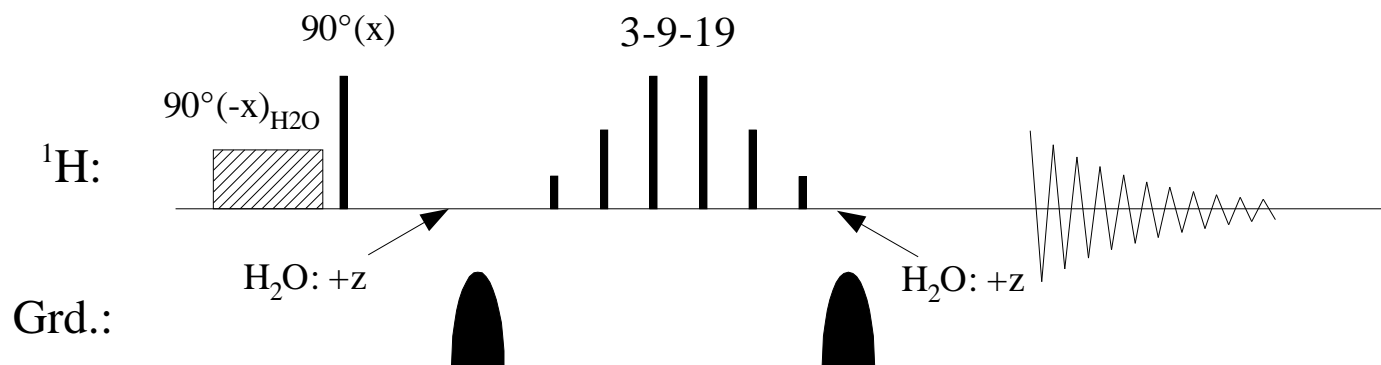
$T_2(\text{H}^N, \text{lysozyme})$ ca. 35 ms —————▶ signal loss of ca. 30% !

Minimal water saturation - Water-flip-back

Signal accumulation faster of the longitudinal relaxation of water results in a saturation transfer of saturated water protons to fast exchanging amide protons.

This results in a reduced signal for fast exchanging protons.

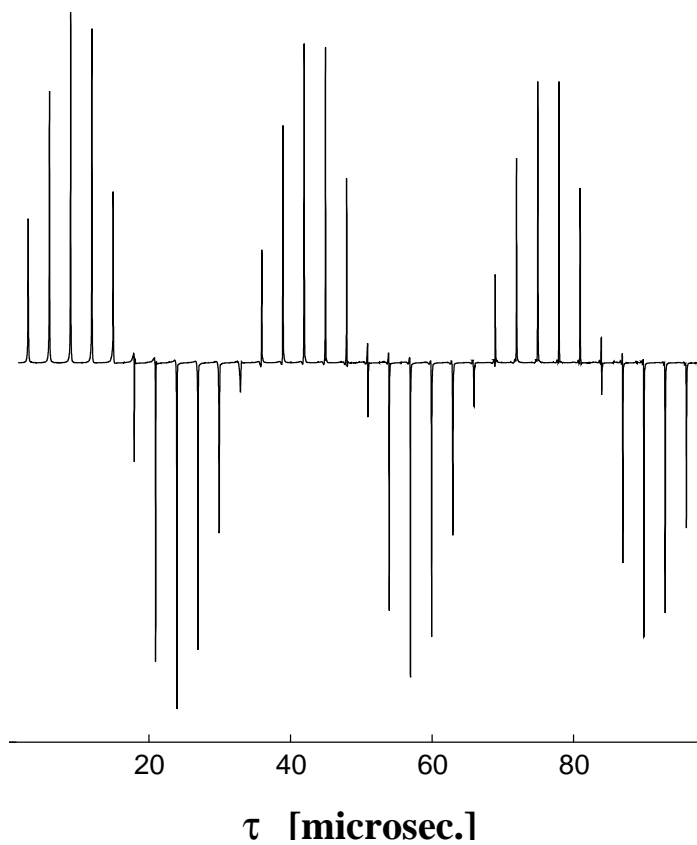
If the applied pulses rotate the water magnetization to $+z$ (equilibrium) at the beginning of the FID, the saturation transfer will be minimized.



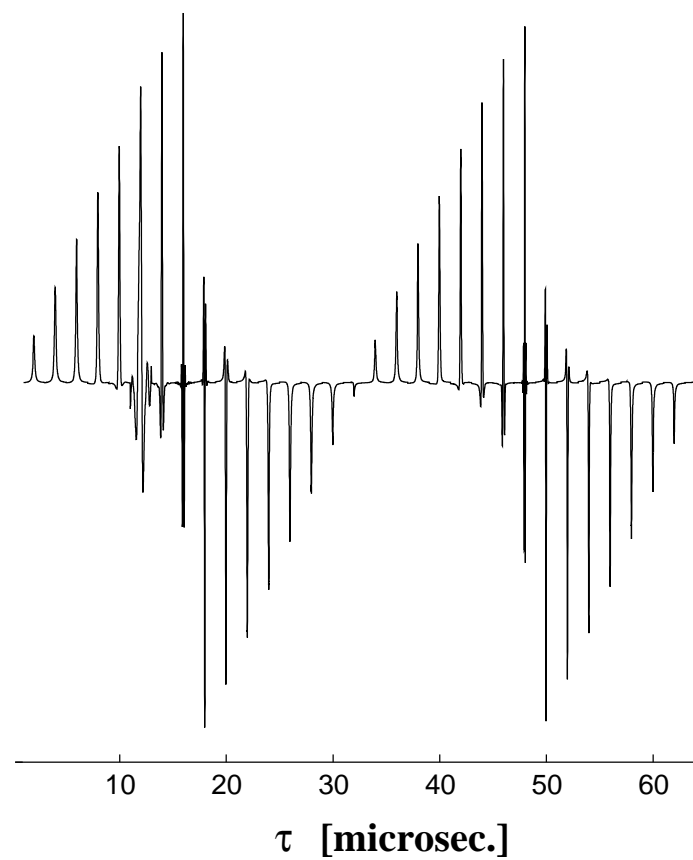
Aqueous samples and radiation damping
 ^1H pulse length calibration

$$\mathbf{I}_z \xrightarrow{\omega_1 \tau \mathbf{I}_y} \mathbf{I}_z \cos(\omega_1 \tau) + \mathbf{I}_x \sin(\omega_1 \tau)$$

1% H₂O in D₂O (400 MHz)

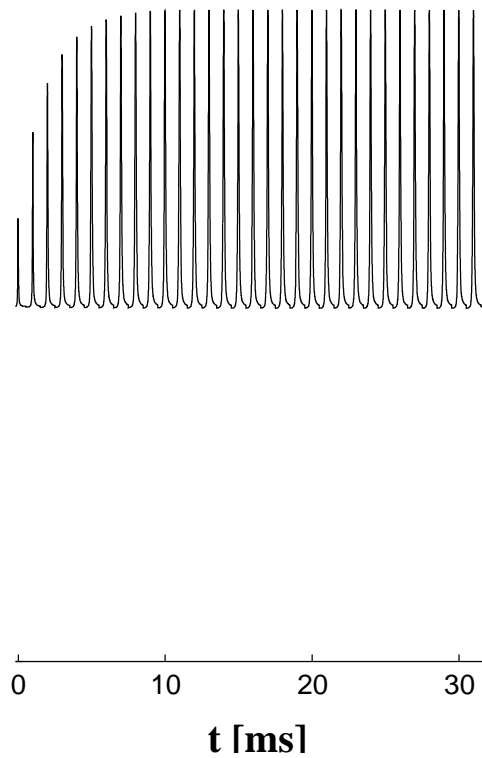


90% H₂O / 10% D₂O (700 MHz)

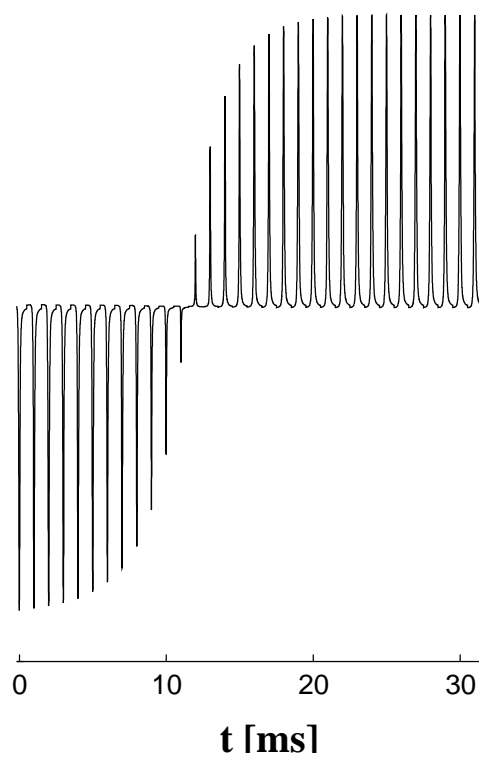


Determination of radiation damping time constant at 700 MHz

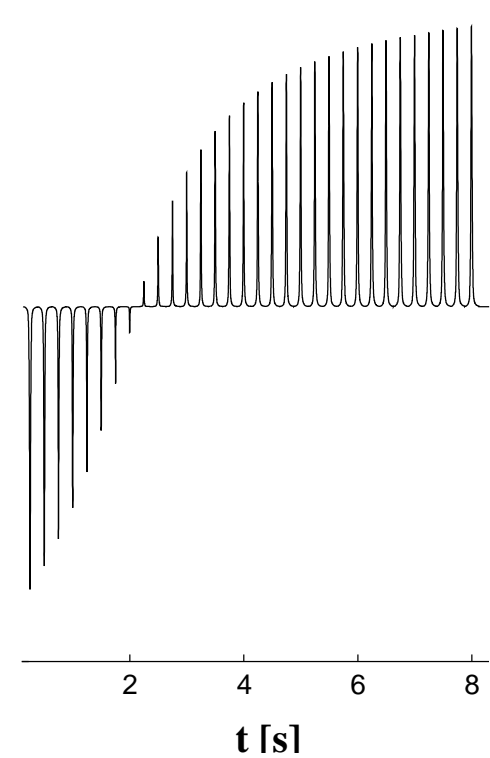
$90^\circ - t - \text{Grad.} - 90^\circ - \text{acq.}$



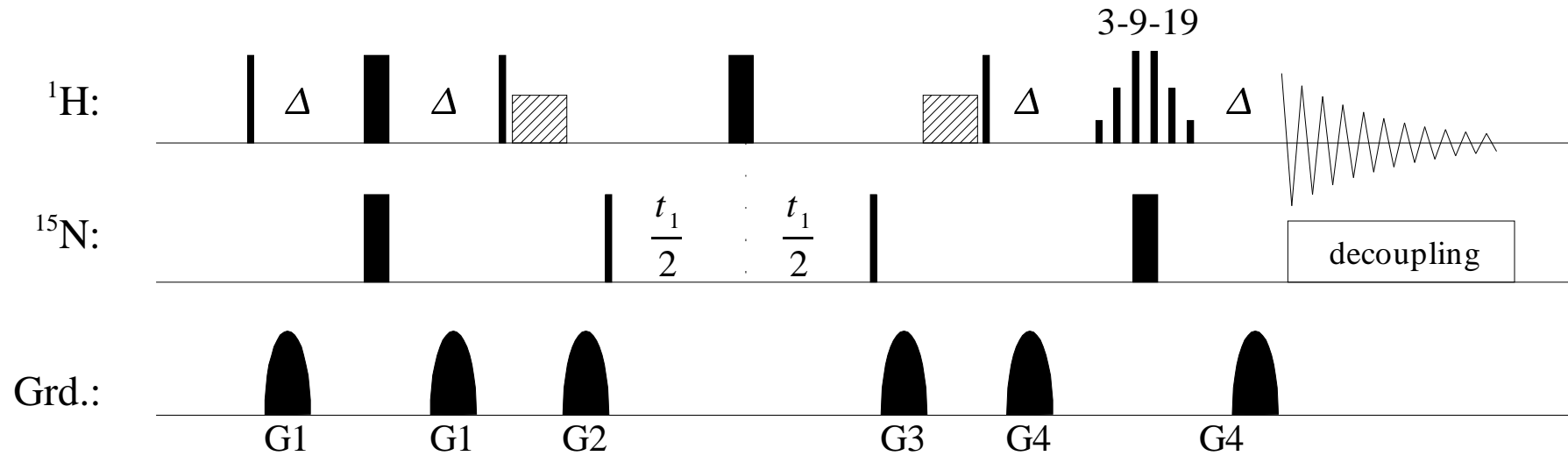
$180^\circ - t - \text{Grad.} - 90^\circ - \text{acq.}$



$180^\circ - t (\text{weak Grad.}) - 90^\circ - \text{acq.}$



Water-flipback in a ^1H , ^{15}N HSQC with selective pulses

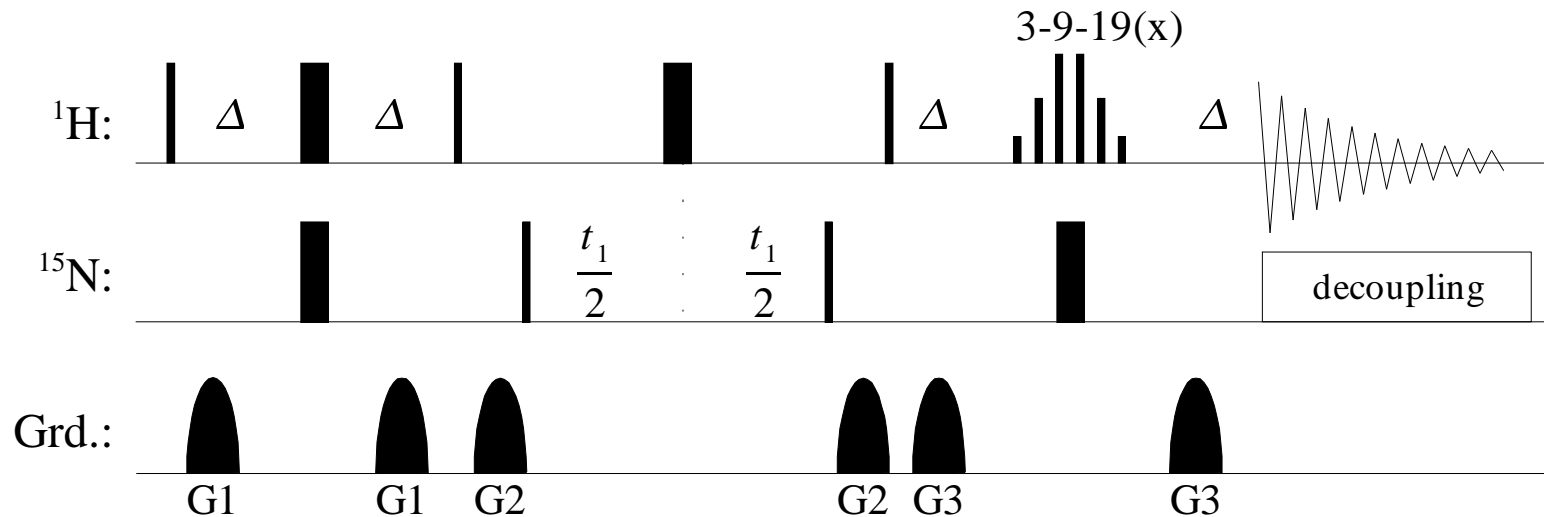


Gradient pairs G1 - 180° (H) - G1 and
 G3 - 180° (H) - G3

suppress radiation damping by dephasing and rephasing of the water magnetization during the INEPT steps

selective water flipback pulse : 2 ms rectangular pulse or shaped pulse

Water-flipback in a ^1H , ^{15}N HSQC without selective pulses (FHSQC, *fast HSQC*)



Gradient pairs G1 - 180° (H) - G1 and
 G2 - 180° (H) - G2

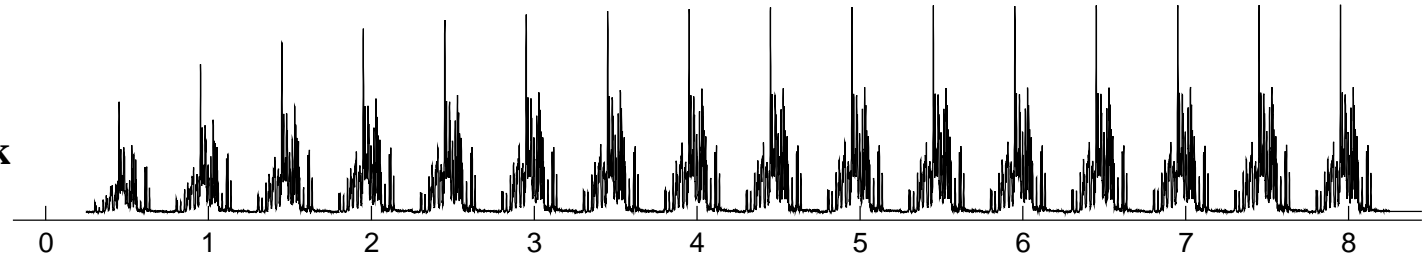
suppress radiation damping by dephasing – rephasing of the water during the INEPT steps and during ^{15}N evolution

^1H pulse phases are chosen that H_2O magnetization is along +z (equilibrium) at the beginning of the FID

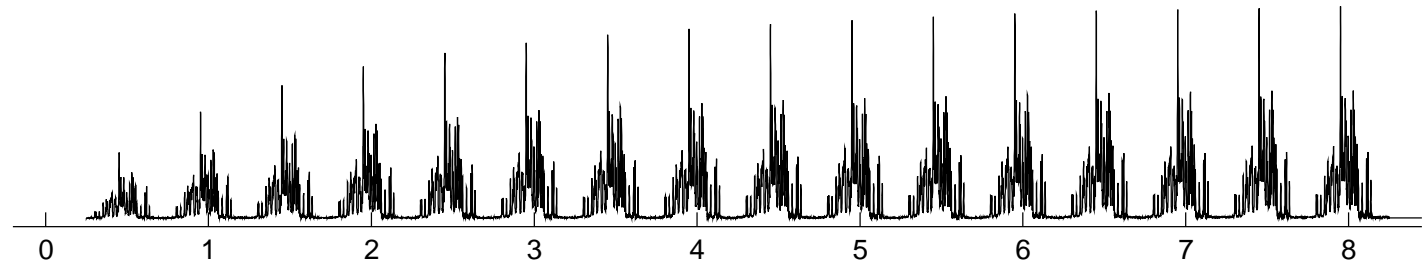
binomial 3-9-19 watergate suppresses residual transverse water magnetization

Different water suppression schemes in 1D ^1H , ^{15}N HSQC experiments

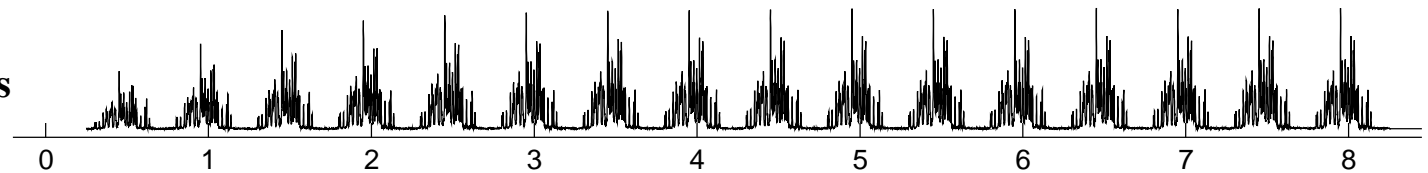
water-flipback



Dephasierung durch Gradienten

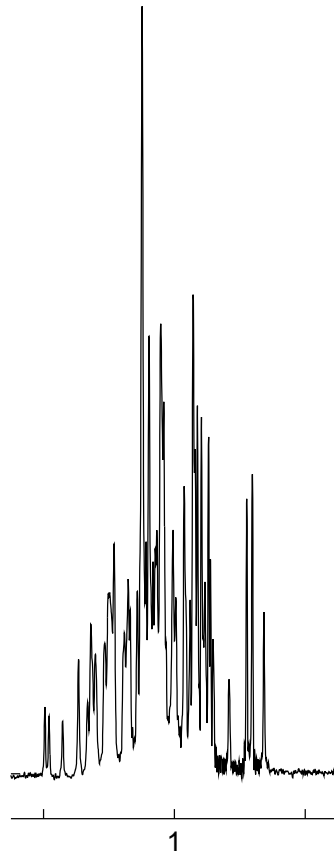


**zusätzliche Vorsättigung
während des Recovery Intervalls**

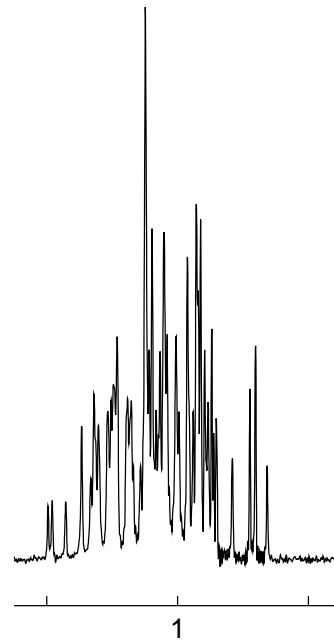


Recovery Intervall [s]

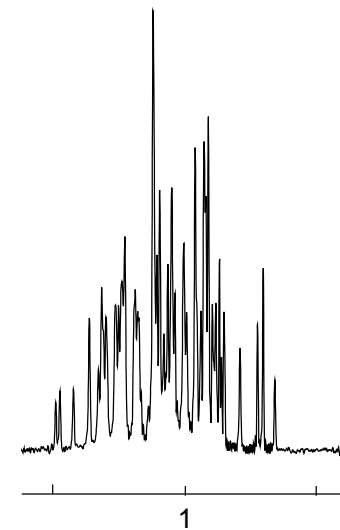
Different water suppression schemes in a 1D ^1H , ^{15}N HSQC with a relaxation delay of 1 sec



water flipback

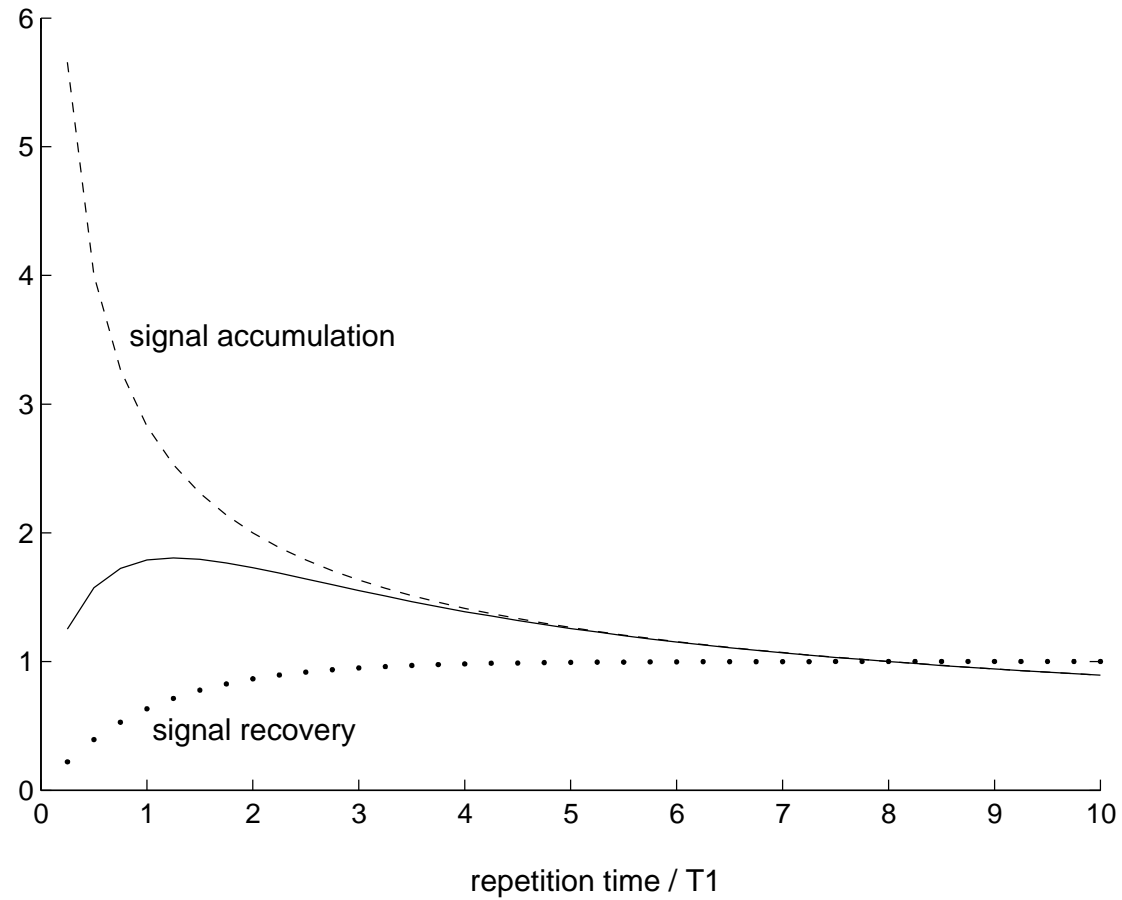


Dephasierung durch Gradienten



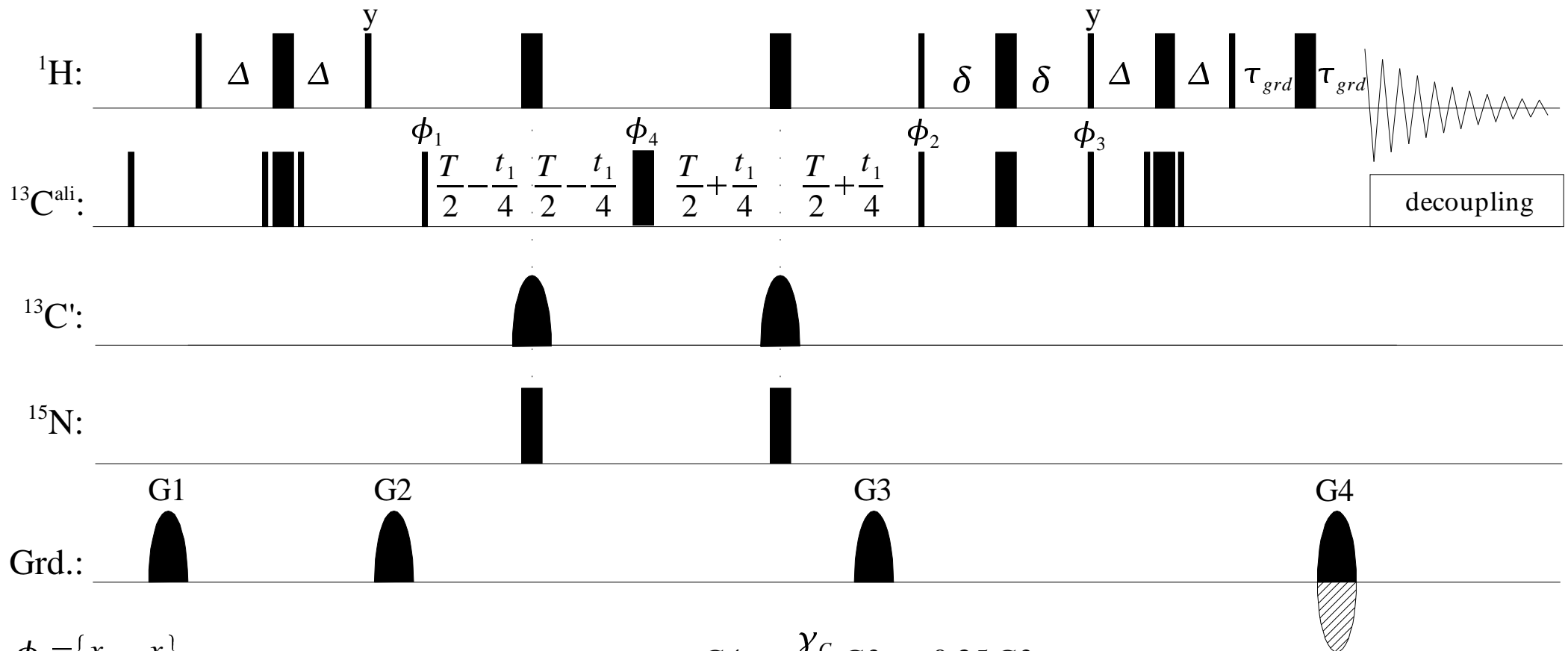
zusätzl. Vorsättigung

Sensitivity of a NMR experiment as function of the repetition rate



→ optimal interscan delay approx. $1.25 \cdot T_1$
(spin diffusion averages proton T_1 in macromolecules)

^1H , ^{13}C constant time HSQC for ^{13}C , ^{15}N labeled proteins



$$\phi_1 = \{x, -x\}$$

$$\phi_2 = \{x, x, -x, -x\}$$

$$\phi_3 = \{y, y, -y, -y\}$$

$$\phi_4 = \{4(x), 4(-x), 4(y), 4(-y)\}$$

$$\phi_{rec} = \{2(x, -x, -x, x), 2(-x, -x, x, -x)\}$$

$$G4 = -\frac{\gamma_c}{\gamma_H} G3 \approx -0.25 G3$$

$$\Delta = 1.7 \text{ ms} \quad ; \quad \delta = 0.8 \text{ ms}$$

Recording of the antiecho : inversion of G4 and ϕ_3

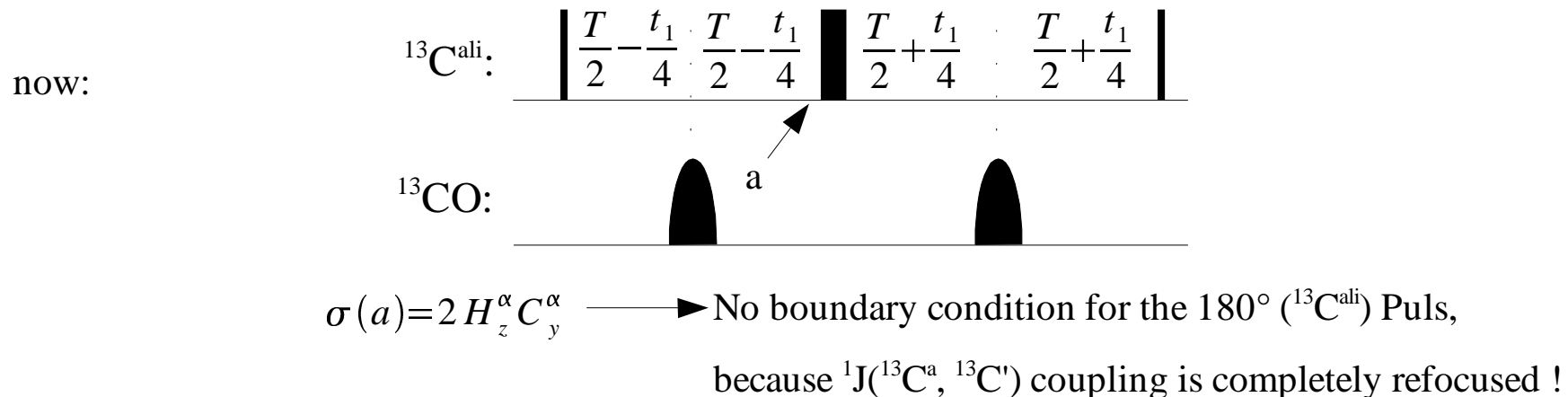
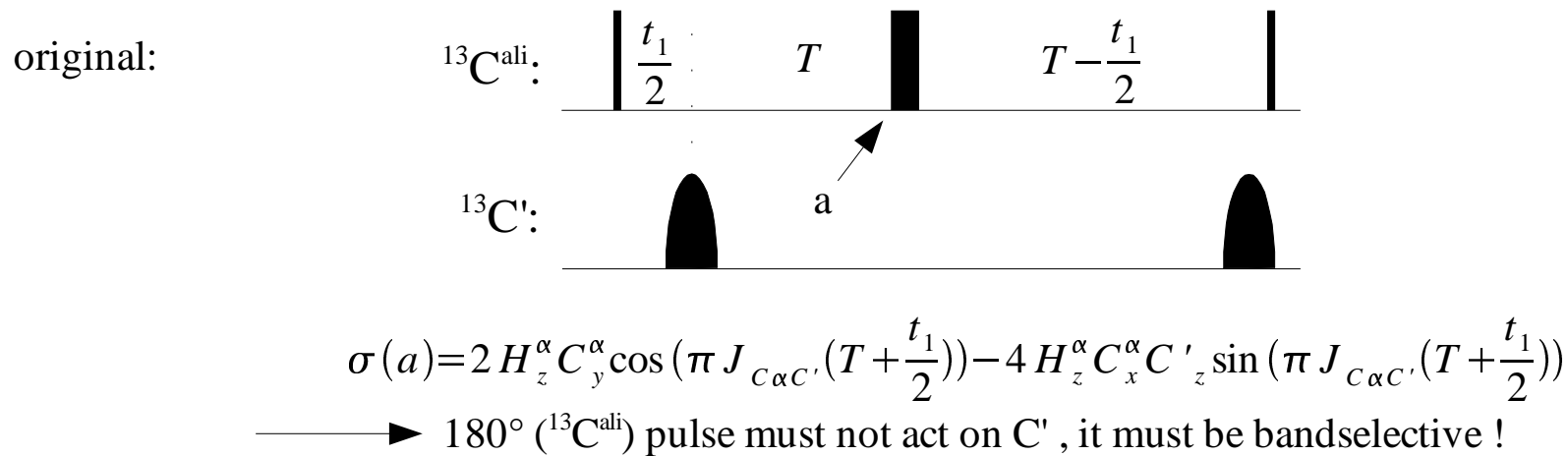
Remarks to the presented pulse sequence

Before the initial INEPT the ^{13}C equilibrium z-magnetization is dephased by $90^\circ(^{13}\text{C})$ - gradient dephasiert.

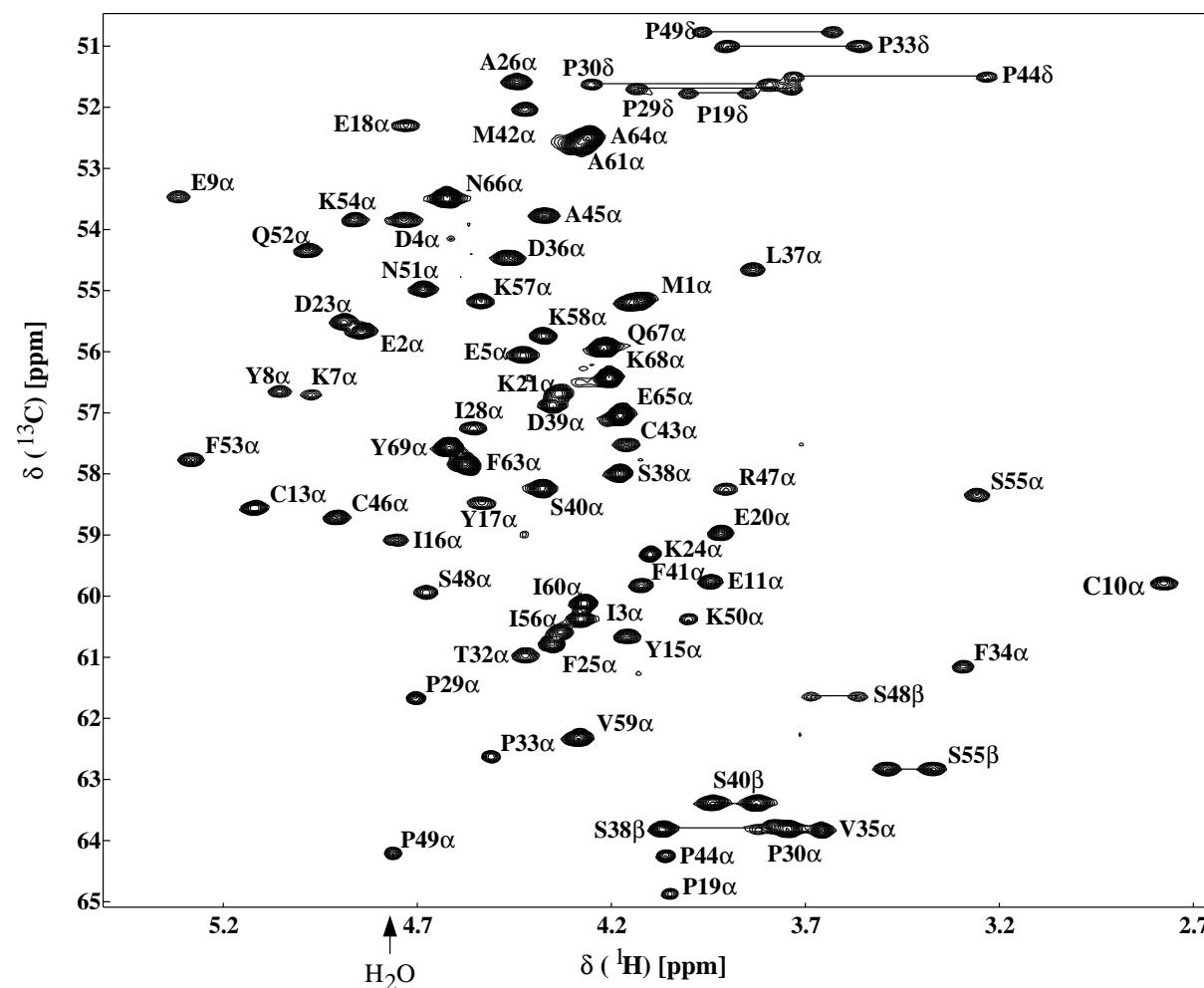
This ensures that no observable magnetization results from this equilibrium magnetization.

The $^1\text{J}(^{13}\text{C}^{\text{a}}, ^{13}\text{C}')$ coupling during the evolution period is refocused by selective $180^\circ(\text{CO})$ pulses.

In the original ct-HSQC these 180° pulses are applied at different time points:



Water suppression in a ^1H , ^{13}C ct-HSQC with gradient selection
 (ca. 2 mM ^{13}C , ^{15}N *G. theta* Rubredoxin (70 aa) in H_2O / D_2O 9:1, 600 MHz)



Intensity of residual t_1 -noise at F2(H_2O) : only 3-5 times the thermal noise level !!